Table 2 Univariate analysis of overall survival

Variable	P-value
EBAG9 immunoreactivity (+ vs −)	0.689
Histological type	0.0177
Histological grade	0.0085
Stage	<0.0001
Residual tumour	<0.0001

Table 3 Association between EBAG9 immunoreactivity and RT–PCR

		EBAG9 immunoreactivity	
		+	−
EBAG9 mRNA	+	16	4
	−	0	2
ERα mRNA	+	9	2
	−	0	6

were positive for ERα mRNA ($n=11$), they were also positive for EBAG9 mRNA (Figure 2).

The result of immunoblotting is shown in Figure 3. Immunoreactive bands corresponding to EBAG9 and ERα were detected in 11 out of 12 and 10 out of 12 of ovarian cancer cell lines, respectively. JHOS2, which was negative for EBAG9, was also negative for ERα.

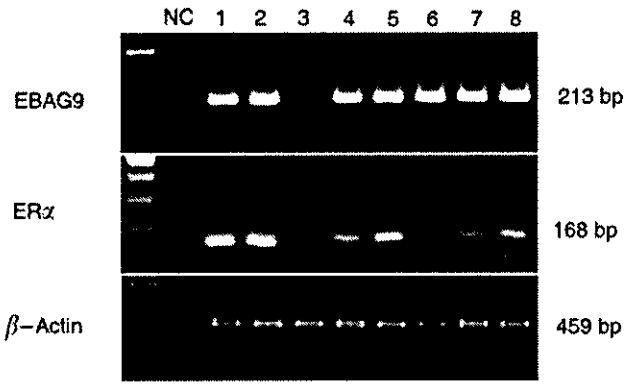

Figure 2 Representative results of RT–PCR for total RNA extracted from epithelial ovarian carcinoma tissues. Bands of the correct size for EBAG9 (213 bp), ERα (168 bp) and β-actin (459 bp) were detected in each histological subtype of ovarian cancer (1,2: serous; 3,4: mucinous; 5,6: endometrioid; 7,8: clear cell). β-Actin was used as a positive control and NC as a negative control. Note that all of the cases that were positive for ERα mRNA were also positive for EBAG9 mRNA.

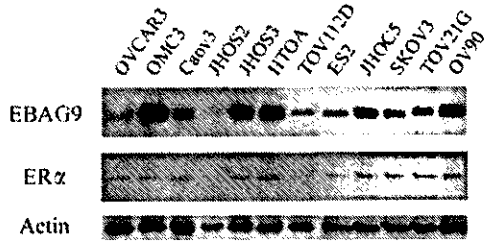

Figure 3 Results of immunoblotting of ovarian cancer cell lines are shown. Actin was used as internal positive controls.

DISCUSSION

In the present study, EBAG9 immunoreactivity was detected in 46 out of 90 epithelial ovarian carcinomas (51.1%). The expression of EBAG9 was significantly associated with advanced disease, although it turned out not to be correlated with prognosis.

It is well recognised that human cancer tissues are infiltrated with tumour-infiltrating lymphocytes (TIL) (Balch *et al*, 1990), a phenomenon known to be a manifestation of the host immune reaction to cancer cells (Rosenberg, 1996). Tumour-infiltrating lymphocytes has been reported to be associated with improved prognosis of some carcinomas, including lung (DiPaola *et al*, 1977) and colon (Naito *et al*, 1998) carcinomas. In ovarian tumour, the degree of lymphocyte infiltration was reported to be associated with the patients' survival rate, clinical stage, grade and histological type (Ma and Gu, 1991). Nakashima *et al* (1999) recently reported that activated CD3+ T lymphocytes express a putative receptor for EBAG9/RCAS1. This receptor expression was enhanced by activation of the lymphocytes, and when these receptor-positive cells were cultured with EBAG9/RCAS1 peptides, their growth was strongly suppressed, and they were eventually led to cell death by apoptosis (Nakashima *et al*, 1999). In breast carcinoma, EBAG9 immunoreactivity was inversely associated with the degree of intratumoral infiltration of mononuclear cells or CD3+ T lymphocytes (Suzuki *et al*, 2001). These results suggested that tumour cells might have evaded immune surveillance by expressing EBAG9/RCAS1, which suppressed clonal expansion and induced apoptosis of receptor-positive immune cells. Although the precise mechanism of immune evasion remains uncertain, the expression of EBAG9/RCAS1 may be a factor related to the escape mechanism of cancer cells from the host immune system.

Several authors reported that expression of RCAS1 was associated with poor prognosis and/or advanced disease in human cancer. Izumi *et al* (2001) reported that RCAS1 expression was positive for 48 of 102 non-small-cell lung carcinoma patients (47.1%) and was significantly correlated with advanced stage, poor differentiation and poor prognosis. Ito *et al* (2003) reported that RCAS1 overexpression was more frequently observed in anaplastic carcinomas than well-differentiated carcinoma in thyroid cancer. In pancreatic ductal adenocarcinoma, RCAS1 expression was demonstrated in 77 of 80 cases (96%) and was an independent prognostic factor (Hiraoka *et al*, 2002). In gynaecological malignancies, Kaku *et al* (1999) reported that patients with high RCAS1 expression showed significantly worse overall survival than those with low expression in adenocarcinoma of uterine cervix. In addition, Sonoda *et al* (1998) reported that RCAS1 was not detected in the normal uterine cervix or ovarian tissue, but strongly expressed in uterine endometrial adenocarcinomas, ovarian adenocarcinomas (Sonoda *et al*, 1996; Sonoda *et al*, 2000) and cervical squamous cell carcinomas. Recently, Suzuki *et al* (2001) reported that EBAG9 immunoreactivity was detected in 82 of 91 in breast carcinoma (90.1%), although it was not associated with clinicopathological parameters. Others reported that EBAG9 gene was consistently expressed in breast cancer cell line, and might play a specific role in early stages of breast carcinogenesis (Tsuneizumi *et al*, 2001). To our knowledge, this is the first report that evaluated the relationships between EBAG9/RCAS1 and clinicopathological parameters in epithelial ovarian cancer. Our results, together with previous reports, suggest that ovarian cancer that expresses EBAG9 may have invasive and progressive characteristics.

There was a strong correlation between EBAG9 and ERα immunoreactivity in ovarian cancer tissues ($P<0.0001$) and cell lines in this study. Also, EBAG9 immunoreactivity was associated with serous histology. Moreover, all of the cases that were positive for ERα mRNA, were also positive for EBAG9 mRNA, suggesting

that the regulation of EBAG9 may be under oestrogen control in ovarian epithelial carcinoma. Oestrogen receptor-binding fragment associated gene 9 was isolated utilising a genomic-binding site cloning method from a cDNA library of MCF-7 human breast cancer cell (Watanabe *et al*, 1998), which expresses ERα and low level of ERβ (Vladusic *et al*, 2000). Transfection analyses have demonstrated that the nucleotide sequences between −86 and −36 contains an ERE in the 5′-promoter region of the EBAG9 gene (Ikeda *et al*, 2000). mRNA levels of EBAG9 in MCF-7 cells are significantly increased within 6 h of oestrogen treatment, an effect that is mediated by the binding of ERα to the ERE in the promoter of the EBAG9 gene (Ikeda *et al*, 2000). On the other hand, Quinn *et al* (1982) reported that serous tumours were more frequently ER-positive than other types of cancers. Results from our present study are consistent with these previous reports, and suggest that EBAG9 is widely distributed in carcinoma cells of human epithelial ovarian carcinoma tissues and cells, maybe especially in serous histology, as a result of oestrogen actions through ER.

In conclusion, the wide distribution of EBAG9 and its relation to advanced disease suggest that this protein may play important roles in epithelial ovarian cancer. Further investigations are required to clarify the precise functions of EBAG9 in epithelial ovarian cancer.

ACKNOWLEDGEMENTS

This work was supported in part by a grant-in-aid for Scientific Research from the Ministry of Health and Welfare, a grant-in-aid from the Ministry of Education, Science and Culture, a grant-in-aid from Kurokawa Cancer Research Foundation and a grant-in-aid from Japan Gynaecologic Oncology Group (JGOG).

REFERENCES

Akahira J, Suzuki T, Ito K, Darnel AD, Moriya T, Sato S, Yaegashi N, Okamura K, Sasano H (2001) Expression of 5α-reductases in human epithelial ovarian cancer: its correlation with androgen receptor status. *Jpn J Cancer Res* **92:** 926–932

Akahira J, Suzuki T, Ito K, Kaneko C, Darnel AD, Moriya T, Okamura K, Yaegashi N, Sasano H (2002) Differential expression of progesterone receptor isoforms A and B in the normal ovary, and in benign, borderline, and malignant ovarian tumors. *Jpn J Cancer Res* **93:** 807–815

Akahira JI, Yoshikawa H, Shimizu Y, Tsunematsu R, Hirakawa T, Kuramoto H, Shiromizu K, Kuzuya K, Kamura T, Kikuchi Y, Kodama S, Yamamoto K, Sato S (2001) Prognostic factors of stage IV epithelial ovarian cancer: a multicenter retrospective study. *Gynecol Oncol* **81:** 398–403

Balch CM, Riley LB, Bae YJ, Salmeron MA, Platsoucas CD, von Eschenbach A, Itoh K (1990) Patterns of human tumor-infiltrating lymphocytes in 120 human cancers. *Arch Surg* **125:** 200–205

Benraad THJ, Friberg CG, Koenders AJM, Kullander S (1980) Do estrogen and progesterone receptors (ER and PR) in metastasizing endometrial cancer predict response to estrogen therapy. *Acta Obstet Gynecol Scand* **59:** 155–159

Bizzi A, Codegoni AM, Landoni F (1988) Steroid receptors in epithelial ovarian cancer: relation to clinical parameters and survival. *Cancer Res* **48:** 6222–6226

DiPaola M, Bertolotti A, Colizza S, Coli M (1977) Histology of bronchial carcinoma and regional lymph nodes as putative immune response of the host to the tumor. *J Thorac Cardiovasc Surg* **73:** 531–537

Ehrlich CE, Young PLM, Cleary RE (1981) Cytoplasmic progesterone and estradiol receptors in normal, hyperplastic and carcinomatous endometria: therapeutic implications. *Am J Obstet Gynecol* **141:** 539–546

Hempling RE, Piver MS, Eltabbakh GH, Recio FO (1998) Progesterone receptor status is a significant prognostic variable of progression-free survival in advanced epithelial ovarian cancer. *Am J Clin Oncol* **21:** 447–451

Hiraoka K, Hida Y, Miyamoto M, Oshikiri T, Suzuoki M, Nakakubo Y, Shinohara T, Itoh T, Shichinohe T, Kondo S, Kasahara N, Katoh H (2002) High expression of tumor-associated antigen RCAS1 in pancreatic ductal adenocarcinoma is an unfavorable prognostic marker. *Int J Cancer* **99:** 418–423

Ikeda K, Sato M, Tsutsumi O, Tsuchiya F, Tsuneizumi M, Emi M, Imoto I, Inazawa J, Muramatsu M, Inoue S (2000) Promoter analysis and chromosomal mapping of human EBAG9 gene. *Biochem Biophys Res Commun* **273:** 654–660

Ito Y, Yoshida H, Nakano K, Kobayashi K, Yokozawa T, Hirai K, Matsuzuka F, Matsuura N, Kuma K, Miyauchi A (2003) Overexpression of human tumor-associated antigen, RCAS1, is significantly linked to dedifferentiation of thyroid carcinoma. *Oncology* **64:** 83–89

Izumi M, Nakanishi Y, Yoshino I, Nakashima M, Watanabe T, Hara N (2001) Expression of tumor-associated antigen RCAS1 correlates significantly with poor prognosis in nonsmall cell lung carcinoma. *Cancer* **92:** 446–451

Kaku T, Sonoda K, Kamura T, Hirakawa T, Sasaki K, Amada S, Ogawa S, Kobayashi H, Nakashima M, Watanabe T, Nakano H (1999) The prognostic significance of tumor-associated antigen 22-1-1 expression in adenocarcinoma of the uterine cervix. *Clin Cancer Res* **5:** 1449–1453

Kaupilla A (1984) Progestin therapy of endometrial, breast and ovarian carcinoma: a review of clinical observations. *Acta Obstet Gynecol Scand* **63:** 441–450

Ma D, Gu MJ (1991) Immune effect of tumor-infiltrating lymphocytes and its relation to the survival rate of patients with ovarian malignancies. *J Tongji Med Univ* **11:** 235–239

Masood S, Heitmann J, Nuss RC, Benrubi GI (1989) Clinical correlation of hormone receptor status in epithelial ovarian cancer. *Gynecol Oncol* **34:** 57–60

McGuire WL (1978) Steroid receptors in human breast cancer. *Cancer Res* **38:** 4289–4291

Naito Y, Saito K, Shiiba K, Ohuchi A, Saigenji K, Nagura H, Ohtani H (1998) CD8+ T cells infiltrated within cancer cell nests as a prognostic factor in human colorectal cancer. *Cancer Res* **58:** 3491–3494

Nakakubo Y, Hida Y, Miyamoto M, Hashida H, Oshikiri T, Kato K, Suzuoki M, Hiraoka K, Ito T, Morikawa T, Okushiba S, Kondo S, Katoh H (2002) The prognostic significance of RCAS1 expression in squamous cell carcinoma of the oesophagus. *Cancer Lett* **177:** 101–105

Nakashima M, Sonoda K, Watanabe T (1999) Inhibition of cell growth and induction of apoptotic cell death by the human tumor-associated antigen RCAS1. *Nat Med* **5:** 938–942

Quinn MA, Pearce P, Rome R, Funder JW, Fortune D, Pepperell RJ (1982) Cytoplasmic steroid receptors in ovarian tumours. *Br J Obstet Gynaecol* **89:** 754–759

Rao BR, Slotman BJ (1991) Endocrine factors in common epithelial ovarian cancer. *Endocr Rev* **12:** 14–26

Rosenberg SA (1996) The immunotherapy of solid cancers based on cloning the genes encoding tumor-rejection antigens. *Ann Rev Med* **47:** 481–491

Sasano H, Frost AR, Saitoh R, Harada N, Poutanen M, Vihko R, Bulin SE, Silverberg SG, Nagura H (1996) Aromatase and 17b-hydroxysteroid dehydrogenase type 1 in human breast carcinoma. *J Clin Endoclinol Metab* **81:** 4042–4046

Sevelda P, Denison U, Schemper M, Spona J, Vavra N, Salzer H (1990) Oestrogen and progesterone receptor contents as a prognostic factor in advanced epithelial ovarian carcinoma. *Br J Obstet Gynecol* **97:** 706–712

Shimizu Y, Kamoi S, Amada S, Hasumi K, Akiyama F, Silverberg SG. (1998) Toward the development of a universal grading system for ovarian epithelial carcinoma. I. Prognostic significance of histopathologic features-problems involved in the architectural grading system. *Gynecol Oncol* **70:** 2–12

Sonoda K, Kaku T, Hirakawa T, Kobayashi H, Amada S, Sakai K, Nakashima M, Watanabe T, Nakano H (2000) The clinical significance of tumor-associated antigen RCAS1 expression in the normal, hyperplastic, and malignant uterine endometrium. *Gynecol Oncol* **79:** 424–429

Sonoda K, Kaku T, Kamura T, Nakashima M, Watanabe T, Nakano H (1998) Tumor-associated antigen 22-1-1 expression in the uterine cervical squamous neoplasias. *Clin Cancer Res* **4:** 1517–1520

Sonoda K, Nakashima M, Kaku T, Kamura T, Nakano H, Watanabe T (1996) A novel tumor-associated antigen expressed in human uterine and ovarian carcinomas. *Cancer* **77**: 1501–1509

Suzuki T, Inoue S, Kawabata W, Akahira J, Moriya T, Tsuchiya F, Ogawa S, Muramatsu M, Sasano H (2001) EBAG9/RCAS1 in human breast carcinoma: a possible factor in endocrine-immune interactions. *Br J Cancer* **85**: 1731–1737

Tsuchiya F, Ikeda K, Tsutsumi O, Hiroi H, Momoeda M, Taketani Y, Muramatsu M, Inoue S (2001) Molecular cloning and characterization of mouse EBAG9, homolog of a human cancer associated surface antigen: expression and regulation by estrogen. *Biochem Biophys Res Commun* **1**: 2–10

Tsuneizumi M, Emi M, Nagai H, Harada H, Sakamoto G, Kasumi F, Inoue S, Kazui T, Nakamura Y (2001) Overrepresentation of the EBAG9 gene at 8q23 associated with early-stage breast cancers. *Clin Cancer Res* **7**: 3526–3532

Vladusic EA, Hornby AE, Guerra-Vladusic FK, Lakins J, LupuR (2000) Expression and regulation of estrogen receptor beta in human breast tumors and cell lines. *Oncol Rep* **7**: 157–167

Watanabe T, Inoue S, Hiroi H, Orimo A, Kawashima H, Muramatsu M (1998) Isolation of estrogen-responsive genes with a CpG island library. *Mol Cell Biol* **18**: 442–449

World Health Organization (1979) *Handbook for Reporting Results of Cancer Treatment*, WHO publication no. 48. Geneva, Switzerland: World Health Organization

Available online at www.sciencedirect.com
SCIENCE DIRECT®
Biochemical and Biophysical Research Communications 319 (2004) 795–800
BBRC
www.elsevier.com/locate/ybbrc

14-3-3σ is down-regulated in human prostate cancer

Tomohiko Urano,[a] Satoru Takahashi,[b] Takashi Suzuki,[c] Tetsuya Fujimura,[b] Masayo Fujita,[a] Jinpei Kumagai,[b] Kuniko Horie-Inoue,[d] Hironobu Sasano,[c] Tadaichi Kitamura,[b] Yasuyoshi Ouchi,[a] and Satoshi Inoue[a,d,*]

[a] *Department of Geriatric Medicine, Graduate School of Medicine, The University of Tokyo, 7-3-1 Hongo, Bunkyo-ku, Tokyo 113-8655, Japan*
[b] *Department of Urology, Graduate School of Medicine, The University of Tokyo, 7-3-1 Hongo, Bunkyo-ku, Tokyo 113-8655, Japan*
[c] *Department of Pathology, Tohoku University School of Medicine, 2-1 Seiryo-machi, Aoba-ku, Sendai 980-8575, Japan*
[d] *Research Center for Genomic Medicine, Saitama Medical School, 1397-1 Yamane, Hidaka-shi, Saitama 350-1241, Japan*

Received 28 April 2004
Available online 28 May 2004

Abstract

The 14-3-3σ is a negative regulator of the cell cycle, which is induced by p53 in response to DNA damage. It has been characterized as an epithelium-specific marker and down-regulation of the protein has been shown in breast cancers, suggesting its tumor-suppressive activity in epithelial cells. Here we demonstrate that 14-3-3σ protein is down-regulated in human prostate cancer cell lines, LNCaP, PC3, and DU145 compared with normal prostate epithelial cells. Immunohistochemical analysis of primary prostate cells shows that the expression of 14-3-3σ protein is epithelial cell-specific. Among prostate pathological specimens, >95% of benign hyperplasia samples show significant and diffuse immunostaining of 14-3-3σ in the cytoplasm whereas <20% of carcinoma samples show positive staining. In terms of mechanisms for the down-regulation of 14-3-3σ in prostate cancer cells, hypermethylation of the gene promoter plays a causal role in LNCaP cells as 14-3-3σ mRNA level was elevated by 5-aza-2′-deoxycytidine demethylating treatment. Intriguingly, the proteasome-mediated proteolysis is responsible for 14-3-3σ reduction in DU145 and PC3 cells, as 14-3-3σ protein expression was increased by treatment with a proteasome inhibitor MG132. Furthermore, tumor necrosis factor-related apoptosis-inducing ligand enhances 14-3-3σ gene and protein expression in DU145 and PC3 cells. These data suggest that 14-3-3σ expression is down-regulated during the neoplastic transition of prostate epithelial cells.

Keywords: 14-3-3σ; Prostate cancer; Epithelial cells; Cell cycle; Methylation; Proteasome; Tumor necrosis factor-related apoptosis-inducing ligand

14-3-3 proteins have diverse cellular functions including critical roles in signal transduction pathways and cell cycle regulation [1–3]. Among the seven isoforms of the 14-3-3 family, 14-3-3σ has been most directly linked to tumor development. 14-3-3σ was originally characterized as a human mammary epithelium-specific marker 1 (HME1) [4], which is down-regulated in mammary carcinoma cells. In spite of ubiquitous distribution of most of the 14-3-3 isoforms, 14-3-3σ expression is restricted to epithelial cells and increases during epithelial differentiation [5]. 14-3-3σ functions as a negative regulator of cyclin-dependent kinases (CDKs) [6,7]. Elevated levels of 14-3-3σ enforce a G2/M arrest by sequestering cyclinB1–cdc2 complexes in the cytoplasm [6]. 14-3-3σ also binds to CDK2 and CDK4 in vitro, suggesting that 14-3-3σ may also affect G1/S transition [7]. Overexpression of 14-3-3σ inhibits cell proliferation and prevents anchorage-independent growth of breast cancer cell lines [7]. Independently, the gene was also identified as a p53-inducible gene involved in cell cycle checkpoint control after DNA damage [8]. Therefore, 14-3-3σ is thought to function as a brake that inhibits cell-cycle progression.

Down-regulation of 14-3-3σ can make primary human epithelial cells grow indefinitely in a single step without the need for exogenous oncogenes or oncoviruses, suggesting that the inactivation of 14-3-3σ leads to tumor formation [9]. In mammary carcinomas, it has been revealed that 14-3-3σ is expressed at very low levels

* Corresponding author. Fax: +81-3-5800-6530.
E-mail address: INOUE-GER@h.u-tokyo.ac.jp (S. Inoue).

0006-291X/$ - see front matter © 2004 Elsevier Inc. All rights reserved.
doi:10.1016/j.bbrc.2004.05.056

[4,10]. Inactivation of 14-3-3σ occurs at transcription level as well as at protein level. In cancer, the expression of 14-3-3σ is reduced by p53 gene inactivation or mutation [8] and by silencing of 14-3-3σ gene via methylation of CpG-residues [11]. At the protein level, proteasome-mediated degradation by an E3 ubiquitin ligase Efp has been shown to be responsible for the 14-3-3σ down-regulation in breast cancer cells [12].

In this study, we demonstrate that 14-3-3σ protein is significantly down-regulated in human prostate cancer cells compared with normal prostate primary epithelial cells (PrECs). The expression of 14-3-3σ is regulated at transcriptional level as well as at post-translational level. Furthermore, 14-3-3σ expression levels in prostate cancer cells could be increased by tumor necrosis factor-related apoptosis-inducing ligand (TRAIL), a member of tumor necrosis factor ligand family that induces apoptosis. These results suggest that the reduction of 14-3-3σ expression is a crucial step for prostate tumorigenesis and the potentiation of 14-3-3σ expression using agents with minimal cytotoxity such as TRAIL could provide a therapeutic option for prostate cancer therapy.

Materials and methods

Chemicals and antibodies. A DNA methyltransferase inhibitor 5-aza-2′-deoxycytidine (Aza-C) was purchased from Sigma (St. Louis, MO). MG132 (Z-Leu-Leu-Leu-aldehyde) was from Peptide Institute (Osaka, Japan). TRAIL was from R&D Systems (Minneapolis, MN). Rabbit polyclonal antibodies against 14-3-3ζ, and 14-3-3τ/θ, and goat polyclonal antibody against 14-3-3σ were purchased from Santa Cruz Biotechnology (Santa Cruz, CA).

Cell culture. Primary human prostate epithelial cells (PrECs) and prostate stromal cells were purchased from Clonetics (San Diego, CA). PrEC cells and prostate stromal cells were maintained in Prostate Epithelial Cell Medium (Clonetics) and Stromal Cell Medium (Clonetics) according to the manufacturer's protocol. Human prostate cancer cells LNCaP, DU145, and PC3 were obtained from American Type Culture Collection (Manassas, VA) and maintained in RPMI1640 media supplemented with 2 mM glutamine, 1% nonessential amino acids, 100 U/ml streptomycin, and penicillin, and 10% FCS.

In experiments with demethylation treatment, cells were cultured in the medium containing 5 μM of freshly dissolved Aza-C for 3 days, by replacing the medium every 24 h. For experiments with proteasome-inhibitory treatment, cells were cultured in the medium with 10 μM MG132 for 4 h. In experiments with TRAIL treatment, cells were maintained in the medium containing 50 ng/ml TRAIL for 12 h.

Western blot analysis. Western blot analysis was performed using protein extracts obtained from 4 strains of PrEC, LNCaP, DU145, and PC-3 cells. Briefly, cells were rinsed twice with ice-cold phosphate-buffered saline (PBS) and lysed in Nonidet P-40 lysis buffer (50 mM Tris–HCl [pH 7.4], 150 mM NaCl, 10 mM NaF, 5 mM EDTA, 5 mM EGTA, 2 mM sodium vanadate, 0.5% sodium deoxycholate, 1 mM dithiothreitol [DTT], 1 mM phenylmethylsulfonyl fluoride [PMSF], 2 μg/ml aprotinin, and 0.1% Nonidet P-40), and the lysates were cleared by centrifugation at 15,000*g* for 15 min at 4 °C. Total protein lysate (20 μg) of each cell line was fractionated on sodium dodecyl sulfate (SDS)–12.5% polyacrylamide gels and electrophoretically transferred onto polyvinylidene difluoride (PVDF) membranes (Immobilon, Millipore, Bedford, MA). The membranes were blocked in Tris-buffered saline (TBS) with 5% skim milk for 30 min and then incubated with 5 ml each of diluted purified anti-14-3-3σ, 14-3-3ζ, and 14-3-3τ/θ antibody at room temperature for 3 h. Each membrane was washed in TBS with 0.1% Tween 20 and incubated with 1:5000 diluted horseradish peroxidase-conjugated donkey anti-rabbit or anti-mouse immunoglobulin (Ig)G (Amersham–Pharmacia Biotech, Arlington Heights, IL) at room temperature for 1 h. Bands were visualized with the chemiluminescence-based ECL plus detection system (Amersham–Pharmacia Biotech). The membranes were exposed to X-ray film. All experiments were performed a minimum of 3 times.

Immunocytochemistry and immunohistochemistry. Primary human prostate epithelial cells and stromal cells were fixed by ice-cold acetone/methanol and permeabilized with 0.1% Triton X-100 for 2 min at room temperature. After washing with PBS, cells were blocked with 10% BSA for 30 min, and incubated with anti-14-3-3σ polyclonal antibody for 3 h at room temperature, followed by three-times washing with 0.1% Tween 20 in PBS. Then, cells were incubated then with FITC-conjugated anti-goat IgG (Jackson ImmunoResearch Labolatories, West Grove, PA) for 1 h at room temperature. Nuclear counterstaining was performed using 1 μg/ml 4′, 6′-diamidino-2-phenylindole (DAPI; Sigma).

Immunohistochemical analysis was performed using 108 prostate pathological specimens (benign; $n = 32$, cancer; $n = 76$) at Tokyo University Hospital by avidin–biotin standard method as described [13]. Briefly, 5 mm thick sections were deparaffinized, pre-treated in citric acid solution, washed in PBS, and incubated in 10% normal horse serum for 30 min. This was followed by overnight incubation at 4 °C with goat polyclonal antibody to human 14-3-3σ, which was used as the primary antibody. Secondary antibodies were biotinylated horse anti-goat IgG used at 1:100 dilution. As a negative control, we substituted anti-14-3-3σ antibody with non-specific goat IgG at the same final concentration. Tissues were subsequently washed with PBS and incubated with biotinylated horse anti-goat IgG secondary antibodies for 60 min at a 1:500 dilution. Slides were washed with PBS and peroxide-conjugated streptavidin was added at a 1:500 dilution for 60 min. Diaminobenzidine (0.06%) was used as the chromogen and 1% modified Harris hematoxylin as the counterstain. For immunohistochemical assessment, 2 independent observers evaluated the tissue sections independently. Positive immunostaining in the cytoplasm for 14-3-3σ was defined as positive. Immunoreactivity (IR) score (0–2) was obtained as the sum of the proportion and the intensity of immunoreactivity; score 0, reactive cells were <10%; score 1, reactive cells were 10–50%; and score 2, reactive cells were >50%. For each specimen, 6 fields were selected at random in the invasive margin of the cancer. Cases with discordant results among the investigators were reevaluated.

Methylation-specific PCR for 14-3-3σ. Genomic DNA was treated with sodium bisulfite and analyzed by real-time PCR by using primer sets that cover CG dinucleotide numbers 3, 4, 8, and 9 of 14-3-3σ [11]. Primers specific for methylated DNA were: 5′-TGGTAGTTTTTATG AAAGGCGTC-3′ (sense), 5′-CCTCTAACCGCCCACCACG-3′ (antisense), primers specific for unmethylated DNA were: 5′-ATGGTAG TTTTTATGAAAGGTGTT-3′ (sense), 5′-CCCTCTAACCACCCAC CACA-3′ (antisense). The percentage of 14-3-3σ gene methylation in each cell line was evaluated.

Real-time PCR. Total RNAs were extracted from cells using a ToTALLY RNA Kit (Ambion, Austin, TX). cDNA was synthesized from 1 μg total RNA of prostate cancer cells using a first strand cDNA synthesis kit (Amersham, IL). PCR primers were designed using PRIMER EXPRESS 1.0 software (Applied Biosystems, Foster City, CA).

Primers specific for 14-3-3σ were: 5′-ACGACAAGAAGCGCAT CATTG-3′ (sense), 5′-GGCATCTCCTTCTTGCTGATGT-3′ (antisense). Primers specific for $p16^{Ink4a}$ were: 5′-ACGTGCGCGATGCCT-3′ (sense), 5′-ATGGCCCAGCTCCTCAG-3′ (antisense). Primers specific for human GAPDH were: 5′-GAAGGTGAAGGTCGGA GTC-3′ (sense), 5′-GAAGATGGTGATGGGATTTC-3′ (antisense).

Quantitative PCR was carried out using a 2× master mix composed of the SYBR Green PCR Core Reagents (Applied Biosystems) and

50 nM of each primer. PCR was performed using an ABI Prism 7000 system (Applied Biosystems) with the following sequence: 2 min at 50 °C, 10 min at 95 °C, and 40 cycles of 15 s at 95 °C and 1 min at 60 °C. For each sample, the ratio between the relative amounts of 14-3-3σ or $p16^{Ink4}$ mRNA and GAPDH mRNA was calculated to compensate for variations in quantity or quality of starting mRNA as well as for difference in reverse transcriptase efficiency.

Results

Western blot analysis

We analyzed the expression of 14-3-3 proteins in PrECs and human prostate cancer cell lines (DU145, PC3, and LNCaP) by Western blot analysis. Reduced expression of 14-3-3σ was observed in DU145 and PC3 cells, whereas absence of expression in LNCaP cells (Fig. 1, top panel). In contrast, the levels of other isoforms of 14-3-3 protein including 14-3-3ζ and 14-3-3τ/θ are not basically different among these cells (Fig. 1, middle and bottom panels).

Immunocytochemistry and immunohistochemistry

We next investigated subcellular localization of 14-3-3σ in primary human prostate epithelial and stromal cells by immunocytochemistry. 14-3-3σ immunoreactivity was detected only in the cytoplasm of PrECs (Fig. 2A) but not in prostate stromal cells (Fig. 2C). We also analyzed immunoreactivity of 14-3-3σ in formalin-fixed paraffin-embedded sections derived from 32 cases of benign prostate hyperplasia (BPH) and 76 cases of clinically localized prostatic cancer. Heavy and diffuse immunostaining of 14-3-3σ was observed in the cytoplasm of benign prostate epithelial cells (Fig. 2E). Of 32 benign prostate hyperplasia cases, the immunoreactivity (IR) scores of 14-3-3σ were 2 (high expression) in 8 cases (25.0%), 1 (low expression) in 23 cases (71.9%), and 0 (negative expression) in 1 case (3.1%) (Table 1). Thus, approximately 97% of BPH specimens showed positive expression of 14-3-3σ protein. In contrast, the expression of 14-3-3σ protein is generally low in prostate carcinoma specimens, as exemplified by a sample of

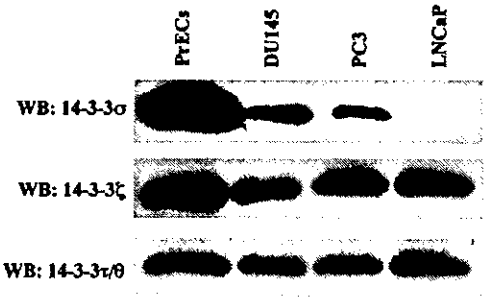

Fig. 1. Western blot analysis of the 14-3-3 proteins in human primary prostate epithelial cells (PrECs) and human prostate cancer cell lines DU145, PC3, and LNCaP. Whole cell extracts were subjected to immunoblotting with anti-14-3-3σ (top), 14-3-3ζ (middle panel), and/or 14-3-3τ/θ (bottom) polyclonal antibody.

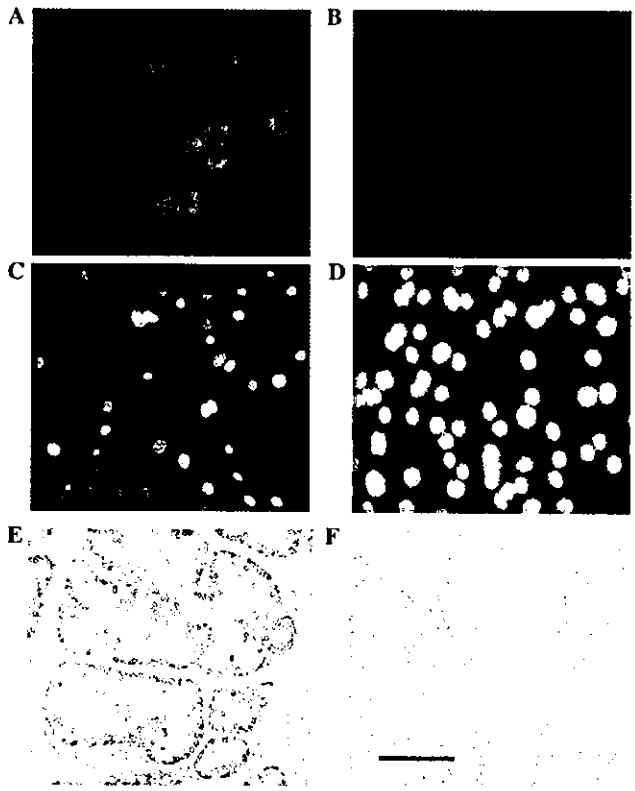

Fig. 2. Reduced expression of the 14-3-3σ protein in human prostate cancer. (A–D) Subcellular localization of 14-3-3σ in human primary prostate cells analyzed by immunohistochemistry. Prostate epithelial cells (A) and stromal cells (B) were stained with anti-14-3-3σ polyclonal antibody. Nuclei were stained with DAPI in prostate epithelial cells (C) and stromal cells (D). (E,F) Representative data from immunohistochemical studies of human benign prostate hyperplasia specimens (E) and prostate cancer specimens (F). Intense and diffuse immunostaining in the cytoplasm is observed in benign prostate epithelial cells (E). No discernible expression of 14-3-3σ was seen in prostate cancer cells of Gleason score 4 tumor (F). Scale bars indicate 100 μm.

Table 1
Immunoreactivity of 14-3-3σ protein in human prostate specimens

14-3-3σ IR score[a]	Prostate status			
	Benign hyperplasia		Prostate cancer	
	No. of cases	Percentage	No. of cases	Percentage
0	1	3.1	61	80.3
1	23	71.9	11	14.4
2	8	25	4	5.3
	32	100	76	100

[a] Immunoreactivity (IR) score (0–2) was obtained as the sum of the proportion and the intensity of immunoreactivity; score 0, reactive cells were <10%; score 1, reactive cells were 10–50%; and score 2, reactive cells were >50%.

Gleason grade 4 tumor with undetectable protein expression in cancerous regions (Fig. 2F). Only <20% of prostate carcinoma specimens showed positive expression of the protein in the cytoplasm. Comparing 14-3-3σ IR scores within single specimens, the cancerous foci showed markedly lower scores than the benign lesions ($p < 0.0001$).

Regulation of 14-3-3σ expression by gene silencing in LNCaP cells

We next assessed which mode of regulation is responsible for down-regulation of 14-3-3σ in prostate cancer cells.

Several lines of evidence demonstrated that hypermethylation of the 14-3-3σ gene occurs in a CpG-rich region (CpG island) that extends from the transcriptional initiation site to the middle of the coding region [11]. Silencing of 14-3-3σ gene by CpG methylation has been found in several tumor types, such as breast and gastric carcinomas [5]. Thus, we investigated whether CpG sites within the 14-3-3σ gene are methylated in prostate cancer cells. Methylation-specific PCR was performed using primers spanning the region between CpG dinucleotides 3 and 9 within the 14-3-3σ gene.

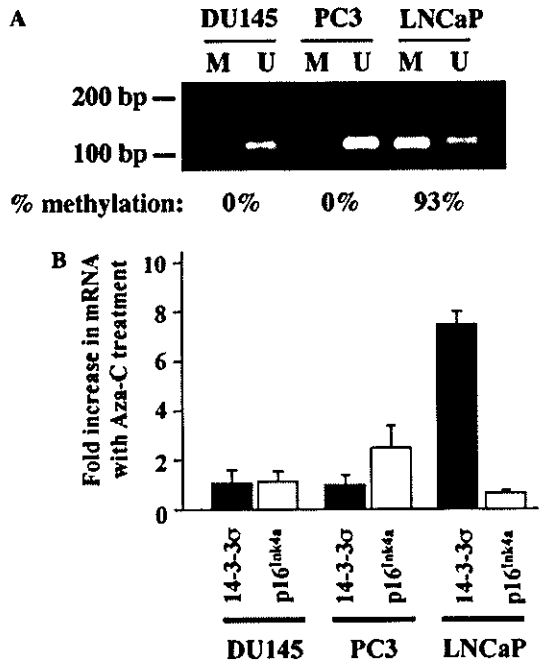

Fig. 3. Methylation status of 14-3-3σ gene in prostate cancer cells. (A) Methylation-specific PCR of 14-3-3σ gene using DNAs from prostate cancer cells. M, methylated DNA; U, unmethylated DNA. (B) Effect of a DNA-demethylating agent 5-aza-2′-deoxycytidine (Aza-C) on the expression of 14-3-3σ and $p16^{Ink4a}$ in prostate cancer cells. Cells were treated with 5 μM Aza-C for 3 days and subjected to RNA extraction. mRNA levels of indicated genes were analyzed by quantitative real-time PCR based on the SYBR Green I methodology and quantified by normalization to GAPDH mRNA levels. Data are presented as fold increase over Aza-C-untreated control of each cell line.

DNAs from DU145 cells and as PC3 cells were completely unmethylated (Fig. 3A). In contrast, DNA from LNCaP cells was predominantly methylated (93%), suggesting a causal role of aberrant methylation in loss of 14-3-3σ expression.

To determine the effect of methylation on 14-3-3σ gene expression, we treated prostate cancer cells with a DNA methyltransferase inhibitor 5-aza-2′deoxycitidine (Aza-C). Treatment of cells with 5 μM Aza-C for 3 days results in a 7-fold elevation of 14-3-3σ gene expression in LNCaP cells while no alteration in DU145 and PC3 cells, as shown by RT-PCR (Fig. 3B). Concomitant methylation of 14-3-3σ and $p16^{Ink4a}$ has been reported in immortalized keratinocytes [9] and oral squamous cell carcinoma [14]. Aza-C treatment activated $p16^{Ink4a}$ gene expression by 2.5-fold in PC3 cells, whereas no association between epigenetic silencing of 14-3-3σ and $p16^{Ink4a}$ was observed in LNCaP cells.

Down-regulation of 14-3-3σ expression by proteasome-dependent pathway in DU145 and PC3 cells

Recently, we have shown that the expression of 14-3-3σ protein is controlled by the proteasomal degradation pathway in breast cancer [12]. Therefore, we tested whether this pathway is involved in the down-regulation of 14-3-3σ in DU145, PC3, and LNCaP cells. Expression of 14-3-3σ protein was markedly increased by treatment with a proteasome inhibitor MG132 in DU145 and PC3 cells. This suggests that the proteasomal degradation pathway is involved in the regulation of 14-3-3σ expression (Fig. 4, left and middle). In contrast, lack of 14-3-3σ protein was not altered by MG132 treatment in LNCaP cells (Fig. 4, right). These results indicate that expression of 14-3-3σ is down-regulated at the post-translational level in DU145 and PC3 cells.

Effect of TRAIL on the expression of 14-3-3σ in prostate cancer cells

Tumor necrosis factor-related apoptosis-inducing ligand is a member of the TNFα superfamily that induces

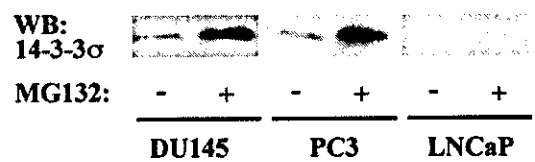

Fig. 4. Proteasome-mediated pathways are responsible for 14-3-3σ down-regulation in DU145 and PC3 cells. Western blot analysis of 14-3-3σ protein expression in prostate cancer cells without or with treatment of a proteasome inhibitor MG132 (10 μM) for 4 h. Immunoblots were probed with anti-14-3-3σ polyclonal antibody. Protein expression of 14-3-3σ was up-regulated with MG132 treatment in DU145 and PC3 cells, while protein expression was undetectable in LNCaP cells.

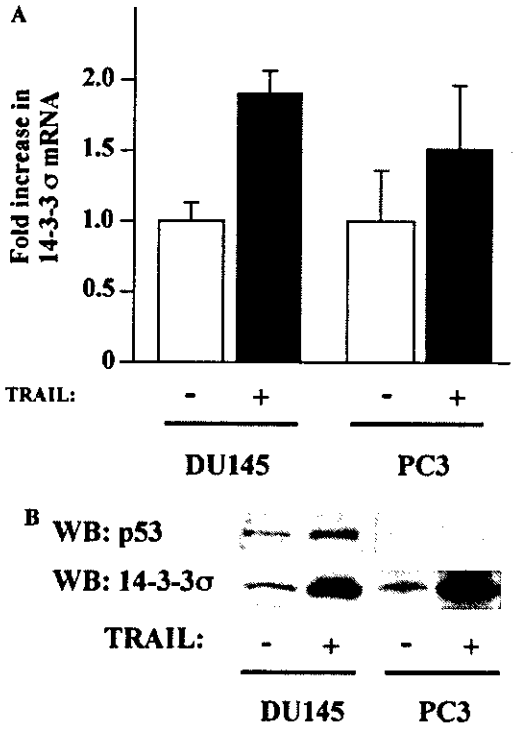

Fig. 5. Effect of tumor necrosis factor-related apoptosis-inducing ligand (TRAIL) on the expression of 14-3-3σ in prostate cancer cells. (A) 14-3-3σ mRNA levels in DU145 and PC3 cells in the absence or presence of TRAIL (50 ng/ml) for 12 h. mRNA levels were quantified as described in Fig. 3B. Data were presented as fold increase over TRAIL-untreated control of each cell line. (B) Western blot analysis of p53 and 14-3-3σ expression in DU145 and PC3 cells without or with TRAIL treatment. Cells were incubated with TRAIL as described in (A). Whole cell extracts were subjected to immunoblotting with anti-p53 monoclonal antibody or anti-14-3-3σ antibody.

apoptosis in prostate cancer cell lines by engaging and activating death receptors [15]. Previous studies showed that 14-3-3σ is up-regulated in response to several apoptotic stimuli [6,8,16,17]. We thus examined whether TRAIL increases 14-3-3σ expression levels in prostate cancer cells. Treatment with TRAIL (50 ng/ml) caused the induction of 14-3-3σ mRNA levels (Fig. 5A) as well as protein levels in both DU145 and PC3 cells (Fig. 5B).

Discussion

In human cells, seven different isoforms of 14-3-3 protein regulate diverse cellular processes by binding to proteins with numerous functions [18]. The σ isoform is predominantly expressed in keratinocytes and breast epithelial cells [4,9]. The expression of 14-3-3σ is directly induced by p53 after DNA damage [8]. Elevated levels of 14-3-3σ enforce a G2/M cell cycle arrest by sequestering cdc2/cyclinB1 complexes in the cytoplasm and are required for a stable G2/M arrest after DNA damage [6]. Furthermore, 14-3-3σ binds to cdk2 and cdk4, suggesting that 14-3-3σ may also affect G1/S progression [7]. In primary keratinocytes, inactivation of 14-3-3σ results in immortalization of the cells [9]. Taken together, previous reports suggest that the inactivation of 14-3-3σ may contribute to tumor formation. Here we demonstrate high expression of 14-3-3σ in human normal prostatic epithelial cells whereas low or null expression in prostate cancer cells. Compared with the expression of σ isoform, the amounts of ζ and τ/θ forms of 14-3-3 protein do not significantly vary between normal prostatic epithelial cells and prostate cancer cells. The present data suggest that the down-regulation of 14-3-3σ could be one of the critical steps in neoplastic transformation of prostatic epithelial cells.

It has been reported that 14-3-3σ expression is silenced by CpG-island methylation in hepatocellular [19], colorectal [20], breast [11], lung [21], and skin basal cell cancers [22]. In the present study, we confirmed that 14-3-3σ mRNA levels in LNCaP cells were increased by demethylating treatment. On the contrary, 14-3-3σ mRNA levels in DU145 and PC3 cells were not altered by demethylation. These data indicate that the down-regulation of 14-3-3σ in prostate cancers is partly due to aberrant methylation of the gene. Alternative pathways such as p53-mediated transcription may also decrease gene expression of 14-3-3σ.

Our results indicate that proteasome-dependent degradation could also play a causal role in the down-regulation of 14-3-3σ in prostate cancer cell lines. Recently, we have shown that an E3 ubiquitin ligase Efp targets 14-3-3σ protein breakdown through proteasome-mediated pathway in breast cancer cells [12]. Therefore, up-regulation of Efp could potentially account for the reduction or loss of 14-3-3σ protein. Further functional analysis of 14-3-3σ together with its E3 ligase may reveal the pathophysiological significance of the proteasome-dependent pathway in prostate tumorigenesis.

14-3-3σ is strongly induced by γ-irradiation and other DNA-damaging agents through p53-dependent pathway. Our data suggest that 14-3-3σ induction is caused also by an apoptotic reagent TRAIL. TRAIL has been reported to induce cell death in a variety of transformed cells including prostate cancer cell lines, DU145 and PC3 [15], but cause little cytotoxicity to normal cells [23]. Here we showed that 14-3-3σ expression was strongly induced by TRAIL in DU145 and PC3 cells. Although 14-3-3σ is a p53-inducible factor, the induction of the protein in DU145 and PC3 cells appears to be p53-independent, as it has been shown that DU145 cells have mutated p53 and PC3 cells do not express functional p53. As TRAIL induces apoptosis as well as could lead to cell cycle arrest through the elevation of 14-3-3σ levels in prostate cancer, TRAIL may have therapeutic potential against advanced prostate cancers regardless of their p53 status.

In summary, we demonstrate that 14-3-3σ is down-regulated in prostate cancer cells. Hypermethylation of

the gene promoter and the proteasome-mediated proteolysis are responsible for the down-regulation of 14-3-3σ. Our data suggest that the reduced or null expression of 14-3-3σ could be closely associated with the acquisition of malignancy in prostate epithelial cells. Additional study of 14-3-3σ function could provide insight into the malignant progression of prostate cancer cells.

References

[1] A. Aitken, 14-3-3 proteins on the MAP, Trends Biochem. Sci. 20 (1995) 95–97.

[2] H. Fu, R.R. Subramanian, S.C. Masters, 14-3-3 proteins: structure, function, and regulation, Annu. Rev. Pharmacol. Toxicol. 40 (2000) 617–647.

[3] W. Wang, D.C. Shakes, Molecular evolution of the 14-3-3 protein family, J. Mol. Evol. 43 (1996) 384–398.

[4] G.L. Prasad, E.M. Valverius, E. McDuffie, H.L. Cooper, Complementary DNA cloning of a novel epithelial cell marker protein, HME1, that may be down-regulated in neoplastic mammary cells, Cell. Growth Differ. 3 (1992) 507–513.

[5] H. Hermeking, The 14-3-3 cancer connection, Nat. Rev. Cancer 12 (2003) 931–943.

[6] T.A. Chan, H. Hermeking, C. Lengauer, K.W. Kinzler, B. Vogelstein, 14-3-3σ is required to prevent mitotic catastrophe after DNA damage, Nature 401 (1999) 616–620.

[7] C. Laronga, H.Y. Yang, C. Neal, M.H. Lee, Association of the cyclin-dependent kinases and 14-3-3σ negatively regulates cell cycle progression, J. Biol. Chem. 275 (2000) 23106–23112.

[8] H. Hermeking, C. Lengauer, K. Polyak, T.C. He, L. Zhang, S. Thiagalingam, K.W. Kinzler, B. Vogelstein, 14-3-3σ is a p53-regulated inhibitor of G2/M progression, Mol. Cell 1 (1997) 3–11.

[9] E. Dellambra, O. Golisano, S. Bondanza, E. Siviero, P. Lacal, M. Molinari, S. D'Atri, M. de Luca, Downregulation of 14-3-3 prevents clonal evolution and leads to immortalization of primary human keratinocytes, J. Cell Biol. 149 (2000) 1117–1130.

[10] A.S. Vercoutter-Edouart, J. Lemoine, X. le Bourhis, H. Louis, B. Boilly, V. Nurcombe, F. Revillion, J.P. Peyrat, H. Hondermarck, Proteomic analysis reveals that 14-3-3σ is down-regulated in human breast cancer cells, Cancer Res. 61 (2001) 76–80.

[11] A.T. Ferguson, E. Evron, C.B. Umbricht, T.K. Pandita, T.A. Chan, H. Hermeking, J.R. Marks, A.R. Lambers, P.A. Futreal, M.R. Stampfer, S. Sukumar, High frequency of hypermethylation at the 14-3-3σ locus leads to gene silencing in breast cancer, Proc. Natl. Acad. Sci. USA 97 (2000) 6049–6054.

[12] T. Urano, T. Saito, T. Tsukui, M. Fujita, T. Hosoi, M. Muramatsu, Y. Ouchi, S. Inoue, Efp targets 14-3-3σ for proteolysis and promotes breast tumour growth, Nature 417 (2002) 871–875.

[13] T. Fujimura, S. Takahashi, T. Urano, S. Ogawa, Y. Ouchi, T. Kitamura, M. Muramatsu, S. Inoue, Differential expression of estrogen receptor β (ERβ) and its C-terminal truncated splice variant ERβcx as prognostic predictors in human prostatic cancer, Biochem. Biophys. Res. Commun. 289 (2001) 692–699.

[14] M. Gasco, A.K. Bell, V. Heath, A. Sullivan, P. Smith, L. Hiller, I. Yulug, G. Numico, M. Merlano, P.J. Farrell, M. Tavassoli, B. Gusterson, T. Crook, Epigenetic inactivation of 14-3-3σ in oral carcinoma: association with p16(INK4a) silencing and human papillomavirus negativity, Cancer Res. 62 (2002) 2072–2076.

[15] R. Yu, S. Mandlekar, S. Ruben, J. Ni, A.N. Kong, Tumor necrosis factor-related apoptosis-inducing ligand-mediated apoptosis in androgen-independent prostate cancer cells, Cancer Res. 60 (2000) 2384–2389.

[16] R. Yoshikawa, M. Kusunoki, H. Yanagi, M. Noda, J.I. Furuyama, T. Yamamura, T. Hashimoto-Tamaoki, Dual antitumor effects of 5-fluorouracil on the cell cycle in colorectal carcinoma cells: a novel target mechanism concept for pharmacokinetic modulating chemotherapy, Cancer Res. 61 (2001) 1029–1037.

[17] T. Samuel, H.O. Weber, P. Rauch, B. Verdoodt, J.T. Eppel, A. McShea, H. Hermeking, J.O. Funk, The G2/M regulator 14-3-3σ prevents apoptosis through sequestration of Bax, J. Biol. Chem. 276 (2001) 45201–45206.

[18] M.J. van Hemert, H.Y. Steensma, G.P. van Heusden, 14-3-3 proteins: key regulators of cell division, signalling and apoptosis, Bioessays 23 (2001) 936–946.

[19] N. Iwata, H. Yamamoto, S. Sasaki, F. Itoh, H. Suzuki, T. Kikuchi, H. Kaneto, S. Iku, I. Ozeki, Y. Karino, T. Satoh, J. Toyota, M. Satoh, T. Endo, K. Imai, Frequent hypermethylation of CpG islands and loss of expression of the 14-3-3σ gene in human hepatocellular carcinoma, Oncogene 19 (2000) 5298–5302.

[20] H. Suzuki, F. Itoh, M. Toyota, T. Kikuchi, H. Kakiuchi, K. Imai, Inactivation of the 14-3-3σ gene is associated with 5′ CpG island hypermethylation in human cancers, Cancer Res. 60 (2000) 4353–4357.

[21] H. Osada, Y. Tatematsu, Y. Yatabe, T. Nakagawa, H. Konishi, T. Harano, E. Tezel, M. Takada, T. Takahashi, Frequent and histological type-specific inactivation of 14-3-3σ in human lung cancers, Oncogene 21 (2002) 2418–2424.

[22] D. Lodygin, A.S. Yazdi, C.A. Sander, T. Herzinger, H. Hermeking, Analysis of 14-3-3σ expression in hyperproliferative skin diseases reveals selective loss associated with CpG-methylation in basal cell carcinoma, Oncogene 22 (2003) 5519–5524.

[23] S.R. Wiley, K. Schooley, P.J. Smolak, W.S. Din, C.P. Huang, J.K. Nicholl, G.R. Sutherland, T.D. Smith, C. Rauch, C.A. Smith, Identification and characterization of a new member of the TNF family that induces apoptosis, Immunity 3 (1995) 673–682.

Geriatrics and Gerontology International 2004; 4: 175–180

ORIGINAL ARTICLE

Association of a single nucleotide polymorphism in the secreted frizzled-related protein 4 (sFRP4) gene with bone mineral density

Masayo Fujita,[1,2] Tomohiko Urano,[1] Masataka Shiraki,[3] Mikio Momoeda,[4] Osamu Tsutsumi,[4] Takayuki Hosoi,[5] Hajime Orimo,[6] Yasuyoshi Ouchi[1] and Satoshi Inoue[1,2]

Departments of [1]Geriatric Medicine and [4]Obstetrics and Gynecology, Graduate School of Medicine, University of Tokyo and [5]Tokyo Metropolitan Geriatric Hospital, Tokyo, [2]Research Center for Genomic Medicine, Saitama Medical School, Saitama, [3]Research Institute and Practice for Involutional Diseases, Nagano, [6]Health Science University, Yamanashi, Japan

Background: Wnt-β-catenin signaling pathway is involved in the regulation of bone mineral density (BMD). Secreted frizzled-related protein (sFRP) 4 that antagonize Wnt signals may modulate Wnt-β-catenin signaling pathway in the bone. Therefore, we analyzed expression of sFRP4 mRNA in primary osteoblasts and the association of a single nucleotide polymorphism (SNP) in the sFRP4 gene with BMD.

Methods: Expression levels of sFRP4 mRNA were analyzed during the culture course of rat primary osteoblasts. Association of a SNP in the sFRP4 gene at Arg262 (CGC to CGT) with BMD was examined in 372 healthy post-menopausal Japanese women.

Results: sFRP4 mRNA was detected and increased during the differentiation of rat primary osteoblasts. As an association study of the SNP in the sFRP4 gene, the subjects without the T allele (CC; $n = 129$) had significantly higher lumbar BMD than the subjects bearing at least one T allele (TT + CT; $n = 243$) (Z score; 0.054 *versus* −0.324; $P = 0.0188$).

Conclusion: sFRP4 mRNA was expressed and regulated in primary osteoblasts. A genetic variation at the sFRP4 gene locus is associated with BMD, suggesting an involvement of sFRP4 gene in the bone metabolism.

Keywords: bone mineral density, osteoblast, osteoporosis, secreted frizzled-related protein 4, single nucleotide polymorphism.

Introduction

Osteoporosis is a multifactorial disorder characterized by low bone mineral density (BMD), increased bone fragility, and increased risk of fracture.[1] Twin and sibling studies have shown that BMD is under genetic control with estimates of heritability ranging from 50% to 90%.[2–4] BMD is regulated by interplay between environmental factors and several genes, each with modest effects on bone mass and bone turnover.[5,6] Several candidate genes have been studied in relation to BMD.[7,8] These include vitamin D receptor (VDR) gene polymorphism,[9] estrogen receptor (ER) gene polymorphism,[10] collagen type Iα1 (COLIA1) gene polymorphism and parathyroid hormone (PTH) gene polymorphism.[11,12] Identification of candidate genes that affect bone mass will be useful for early detection of individuals who are at risk for osteoporosis and early institution of preventive measures.

Accepted for publication 23 March 2004.

Correspondence: Dr Satoshi Inoue MD, Ph. D. Department of Geriatric Medicine, Graduate School of Medicine, University of Tokyo, 7-3-1 Hongo, Bunkyo-ku Tokyo, 113-8655, Japan.
Email: inoue-ger@h.u-tokyo.ac.jp

The Wnts represent a large group of secreted signaling proteins that are involved in cell proliferation and differentiation and play pivotal roles in morphogenesis.[13] It is also known that Wnt and bone morphogenetic protein (BMP) signals control apical ectodermal ridge (AER) formation and dorsal–ventral patterning during limb development.[14,15] Wnt proteins activate signal transduction through Frizzled which act as receptors for Wnt proteins and induce stabilization of cytoplasmic β-catenin protein.[16] Meanwhile, LDL receptor-related protein 5 and 6 (LRP5/6) were also found to be required for Wnt coreceptors.[17,18] Recent reports demonstrated that the Wnt-β-catenin signaling pathway regulates bone density through the LRP5.[19–22] It is also reported that activated β-catenin induced osteoblast differentiation of C3H10T1/2 cells.[23] These findings indicate that Wnt-β-catenin signaling pathway plays important roles in skeletal biology.

Recently, a secreted frizzled-related protein (sFRP) family was described.[24,25] Members of this family share the Wnt binding domain of the Frizzled proteins but lack their 7-transmembrane segments. It has been suggested that these sFRP proteins may control morphogenesis by binding Wnts extra-cellularly and antagonize their ability to signal through the plasma membrane-bound Frizzled receptors.[24,25] sFRP4, one of the sFRP family protein, is found to be expressed in the cartilage and osteoblasts.[26] Therefore, it is possible that sFRP4 modulates Wnt-β-catenin signaling pathway in the bone. In the present study, we examine the sFRP4 mRNA expression in primary osteoblasts and an association between a polymorphism in the sFRP4 gene and BMD in Japanese women to investigate possible contribution of the sFRP4 to bone metabolism.

Materials and methods

Cell culture

Rat primary osteoblasts were isolated from calvaria of 5-day-old-neonatal rats by enzymatic digestion as described previously with some modification.[27] Briefly, calvaria were minced and incubated at 37°C for 20 min in magnesium-free phosphate-buffered saline containing 0.1% collagenase and 0.2% dispase. The enzymatic digestion was repeated twice. The second digestion was performed for 70 min. Cells isolated at second digestion were cultured in α-MEM containing 10% fetal bovine serum (FBS) and antibiotics (100 IU/mL penicillin and 100 mg/mL streptomycin). Cells at the second passage were used for experiments.

Total RNA isolation and cDNA synthesis

Osteoblasts were cultured in 6-cm dishes with α-MEM containing 10% FBS, 50 μg/mL ascorbic acid and 5 mmol/L β-glycerophosphate for 3, 5, 8, 11, 13, 15 or 18 days. Total RNAs were extracted from these cells using a Totally RNA Kit (Ambion, TX). cDNA was synthesized from 1 μg of total RNA of primary osteoblasts using first strand cDNA synthesis kit (Amersham, IL).

SYBR green real time PCR

Primers were designed using Primer Express 1.0 software (Applied Biosystems, CA). Definitive primers were: rat GAPDH forward 5′ -GGCACAGTCAAGGCTGA GAAT- 3′, reverse 5′ -TCGCGCTCCTGGAAGATG- 3′, rat alkaline phosphatase (ALP) forward 5′-TGACCACC ACTCGGGTGAA-3′, reverse 5′-GCATCTCAT-TGTCC GAGTACCA-3′ and rat sFRP4 forward 5′-GT TGAAGCCACCCTTACAGGATA-3′, reverse 5′-GGTC CTAAGGCAAGTGGTGTGT-3′. Polymerase chain reaction (PCR) products were 71 bp, 87 bp and 79 bp length for GAPDH, ALP and sFRP4, respectively. Quantitative PCR was carried out using a 2 × master mix composed from the SYBR Green PCR Core Reagents (Applied Biosystems) and 50 nmol/L primers. PCR reactions were performed using an ABI Prism 7000 system (Applied Biosystems) with the following sequence: 2 min at 50°C, 10 min at 95°C and 40 cycle of 15 s at 95°C and 1 min at 60°C. ALP or sFRP4 signal was normalized to GAPDH signal.

Subjects

Genotypes were analyzed in DNA samples obtained from 372 healthy post-menopausal Japanese women (mean age ± SD; 64.22 ± 9.83) living in Nagano prefecture, Japan. Exclusion criteria included endocrine disorders such as hyperthyroidism, hyperparathyroidism, diabetes mellitus, liver disease, renal disease, use of medications known to affect bone metabolism (e.g. corticosteroids, anticonvulsants, heparin sodium) or unusual gynecologic history. All were non-related volunteers and provided informed consent before this study.

Measurement of BMD and biochemical markers

The lumbar-spine BMD and total body BMD (in g/cm^2) of each participant were measured by dual-energy X-ray absorptiometry using fast-scan mode (DPX-L; Lunar, Madison, WI). We measured serum concentration of calcium (Ca), phosphate (P), alkaline phosphatase (ALP), intact-osteocalcin (I-OC, ELISA; Teijin, Tokyo, Japan), intact parathyroid hormone (PTH), calcitonin (CT), 1, 25(OH)2D3, total cholesterol (TC) and triglyceride (TG). We also measured the urinary pyridinoline (PD, HPLC method) and deoxypyridinoline (DPD, HPLC method). The BMD data were recorded as 'Z scores', that is deviation from the weight-adjusted average BMD for each age. Z scores were calculated using installed software (Lunar DPX-L) on the basis of data from 20 000 Japanese women.

Determination of the sFRP4 genotype

DNA was extracted from peripheral leukocytes by standard techniques. In sFRP4 gene, neither missense mutation nor polymorphism in the promoter region was found from JSNP-database (http://snp.ims.u-tokyo.ac.jp/index.html). Thus, silent mutation for Arg262 (CGC to CGT) of the sFRP4 gene was determined using the TaqMan (Applied Biosystems) PCR method.[28] To determine the sFRP4 SNP, we used Assays-on-Demand SNP Genotyping Products C_1328209_10 (Applied BioSystems), which contain sequence-specific forward and reverse primers and two TaqMan MGB probes for detecting alleles. During the PCR cycle, two TaqMan probes hybridize competitively to a specific sequence of the target DNA, and the reporter dye separate from the quencher dye, resulting in an increase in fluorescence of the reporter. The fluorescence levels of the PCR products were measured with the ABI PRISM 7000 (Applied Biosystems) resulting in clear identification of three genotypes of the SNP.

Statistical analysis

Comparisons of Z scores and biochemical markers between the group of individuals possessing one or two chromosomes of the T-allele and the group with only C-allele encoded at that locus were subjected to statistical analysis (Student's *t*-test; StatView-J 4.5). A *P*-value less than 0.05 was considered statistically significant.

Results

SFRP4 mRNA expression is regulated during the course of primary osteoblasts differentiation

At the inception of this study, we measured sFRP4 mRNA levels during the course of differentiation in rat primary osteoblasts. In the presence of ascorbic acid and β-glycerophosphate, primary osteoblasts proceed through differentiation normally with the deposition of a collagenous extracellular matrix that mineralizes.[29,30] The continual maturation of the osteoblasts was reflected by the increase in ALP mRNA levels (Fig. 1A). sFRP4 mRNA levels exhibited an increase that spanned day 11 to day 18, indicating that the up-regulation of sFRP4 mRNA paralleled with the increase of ALP mRNA expression (Fig. 1B).

Association of sFRP4 gene polymorphism in exon4 with BMD

We analyzed the genotypes for a sFRP4 polymorphism at Arg262 (CGC to CGT) in subjects, using TaqMan methods. Among 372 post-menopausal volunteers, 77 were TT homozygotes, 166 were CT heterozygotes, and 129 were CC homozygotes.

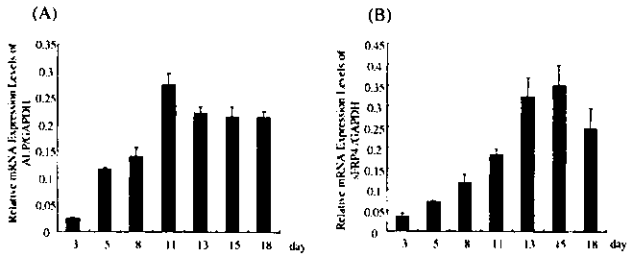

Figure 1 Expressions of ALP and sFRP4 mRNA during culture course of rat primary osteoblasts were analyzed by real time RT-PCR. Rat primary osteoblasts were cultured with α-MEM containing 10% FBS, 50 μg/mL ascorbic acid and 5 mmol/L β-glycerophosphate up to 18 days. At the indicated times, RNA was extracted and the expression levels of ALP (A) and sFRP4 (B) were analyzed by real time PCR, normalized to GAPDH expression (n = 4 for each group). Values are means + SD.

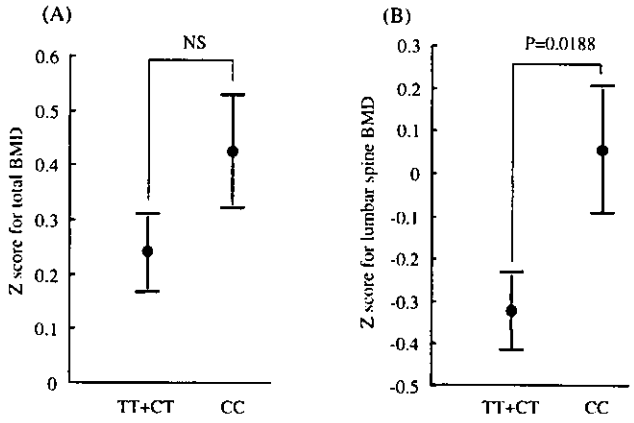

Figure 2 Z score values of total body and lumbar spine bone mineral density (BMD) in the groups with each genotype of sFRP4 polymorphism at Arg262 (CGC to CGT). (A) Z score values for total BMD are shown for genotype TT + CT and for genotype CC. Values are expressed as mean ± SE. Number of subjects are shown in parentheses. (B) Z scores for lumbar BMD as shown in the same manner as (A).

We compared Z scores for BMD of total body and lumbar spine between the subjects bearing at least one T allele (TT + CT) and subjects without the T allele (CC). Comparison of the Z scores of the total BMD between those with and without T allele showed a higher average value for the CC homozygote group, but the difference was not statistically significant (Fig. 2A). On the other hand, Z scores of the lumbar BMD in the CC homozygote group was significantly higher than in the other group (Fig. 2B). Among the biochemical markers examined, ALP was higher in the CC homozygote group than the other group (Table 1). Other than ALP, the background and biochemical data were not statistically different between these groups.

Table 1 Comparison of Z scores of lumbar spine (L2–L4) and total body bone mineral density, background and biochemical data of subjects between the two groups of genotypes

Items	Genotype (mean ± SD) TT + CT	CC	*P*-value
Number of subjects	243	129	
Age (years)	65.18 (9.26)	65.90 (10.45)	NS
Body weight (kg)	50.40 (7.77)	49.93 (8.70)	NS
Body height (cm)	150.11 (6.36)	151.41 (6.21)	NS
Years after menopause	15.97 (9.81)	16.08 (11.06)	NS
Lumbar BMD (g/cm^2)	0.876 (0.183)	0.920 (0.209)	0.0366
Lumbar BMD (Z-score)	−0.324 (1.359)	0.054 (1.659)	0.0188
Total BMD (g/cm^2)	0.971 (0.114)	0.987 (0.112)	NS
Total BMD (Z-score)	0.240 (1.049)	0.426 (1.128)	NS
ALP (IU/L)	186.25 (62.16)	201.18 (71.43)	0.0385
Ca (mg/dL)	9.228 (0.448)	9.202 (0.424)	NS
P (mg/dL)	3.427 (0.473)	3.344 (0.462)	NS
I-OC (ng/mL)	8.012 (3.91)	7.782 (3.126)	NS
PD (pmol/umol of Cr)	35.66 (18.45)	33.25 (13.33)	NS
DPD (pmol/umol of Cr)	7.530 (3.920)	7.397 (2.795)	NS
PTH (pg/mL)	36.05 (16.31)	32.50 (12.64)	NS
CT (pg/mL)	22.67 (11.01)	16.35 (5.91)	NS
1,25-(OH)2D3 (pg/mL)	35.54 (11.48)	36.79 (8.91)	NS
TC (mg/dL)	199.19 (38.84)	198.10 (35.96)	NS
TG (mg/dL)	144.06 (87.13)	133.78 (73.22)	NS
%FAT	32.06 (7.37)	30.29 (8.39)	NS

Values are given as means ± SD.
NS, not significant; BMD, bone mineral density; Ca, calcium; P, phosphate; ALP, alkaline phosphatase; I-OC, intact osteocalcin; PD, pyridinoline; DPD, deoxypyridinoline; PTH, parathyroid hormone; CT, calcitonin; TC, total cholesterol; TG, triglyceride; %FAT, body fat percentage.

Discussion

During the course of primary osteoblast differentiation, the increase of sFRP4 expression was accompanied by the increase of ALP expression, which is a marker of osteoblast differentiation.[31] This result suggests some roles of sFRP4 in the osteoblasts. Recent reports demonstrated that the Wnt-β-catenin signaling pathway regulates bone density through the LRP5. Inactivating mutations in the LRP5 gene decrease bone mass and cause the autosomal-recessive disorder osteoporosis-pseudoglioma syndrome in humans and mice.[19,20] Conversely, activating mutations in the LRP5 gene are linked to autosomal-dominant high bone mass traits.[21,22] Thus, Wnt signaling plays a pivotal role in bone metabolism. Wnt signaling is initiated by binding of Wnts to the Frizzled, and antagonize glycogen synthase kinase 3β (GSK3β)/adenomatous polyposis coli (APC)/Axin complex, leading to the stabilization of β-catenin. Stabilized β-catenin accumulates in the nucleus, interact with lympoid enhancer factor (LEF)-1/T-cell factor (TCF) and activates Wnt target genes.[32] sFRP4, which is assumed to antagonize Wnt signaling, may also regulate Wnt target genes and be involved in bone metabolism.

To our knowledge, the present study is the first to investigate the influence of a polymorphism of the sFRP4 gene on BMD. We demonstrated that the Japanese post-menopausal women who had one or two allele(s) of a synonymous change of C-T transition showed significantly lower lumbar BMD. Total BMD was also lower in the subjects bearing at least one T allele, although the difference was not statistically significant. Lower BMD in post-menopausal women can be considered a result of abnormally rapid bone loss and/or lower peak bone mass. The SNP analyzed in this study would be useful as a genetic marker for low BMD and susceptibility to osteoporosis. Although the biological meanings of this polymorphism should be revealed by functional studies, three hypotheses could be proposed at present. First, silent polymorphism may be linked with other mutations in exons, which contributes to the change of the sFRP4 protein function. Second, SNP may be linked with a mutation in regulatory elements affecting the levels of expression through variable transcriptional regulation. Third, this SNP in the sFRP4 gene may be linked with a mutation of another undefined gene adjacent to the sFRP4 gene that causes low BMD directly or indirectly.

Bone resorption markers showed no significant differences between the genotypes of the sFRP4 gene. In contrast, the serum level of ALP was higher in the CC group, which had significantly higher lumbar BMD. These findings suggested that increased bone formation might be involved in higher BMD. However, the values of osteocalcin were not significantly increased in this group. Although both ALP and osteocalcin are bone formation markers, ALP is an early marker of osteoblast differentiation and osteocalcin is a marker of late osteoblast differentiation.[31] According to the *in vitro* study, β-catenin induced ALP expression but not osteocalcin expression in C3H10T1/2 suggesting that β-catenin might activate early osteoblast differentiation.[23] sFRP4 is thought to be an extracellular antagonist of Wnt signaling, therefore we could speculate that sFRP4 is involved in the regulation of early osteoblast differentiation by modulating the Wnt–β–catenin pathway. However, we measured total ALP in the present study, it is possible that this did not represent a useful parameter for bone formation.

Recently, sFRP4 was shown to be a factor produced by tumors derived from subjects with tumor-induced osteomalacia (TIO).[33] This report suggests that sFRP4 is a circulating protein associated with renal phosphate wasting. Phosphate is a main constituent of the bone matrix and is required for proper bone mineralization. Thus, it is possible that sFRP4 may affect the bone metabolism not only by regulating osteoblastic Wnt-β-signaling, but also by regulating the phosphate metabolism. In the present study, the CC group of the SNP of the sFRP4 gene had significantly high bone density. However, the difference in serum phosphate was not significant between the CC group and the other group. In addition, whether this polymorphism is associated with circulating sFRP4 concentration remains unclear. Further studies will be required to clarify the sFRP4 function in skeletal homeostasis and the biological significance of this polymorphism.

Acknowledgments

We thank Ms. C. Onodera, E. Sekine and M. Kumasaka for expert technical assistance. This work was partly supported by grants from Core Research for Evolutional Science and Technology (CREST), Japan Science and Technology Corporation and the Japanese Ministry of Health, Labor and Welfare and the Japanese Ministry of Education, Science, Sports and Culture.

References

1 Kanis JA, Melton LJ 3rd, Christiansen C, Johnston CC, Khaltaev N. The diagnosis of osteoporosis. *J Bone Miner Res* 1994; **9**: 1137–1141.
2 Flicker L, Hopper JL, Rodgers L, Kaymakci B, Green RM, Wark JD. Bone density determinants in elderly women: a twin study. *J Bone Miner Res* 1995; **10**: 1607–1613.
3 Smith DM, Nance WE, Kang KW, Christian JC, Johnston CC Jr. Genetic factors in determining bone mass. *J Clin Invest* 1973; **2**: 2800–2808.
4 Young D, Hopper JL, Nowson CA *et al.* Determinants of bone mass in 10- to 26-year-old females: a twin study. *J Bone Miner Res* 1995; **10**: 558–567.
5 Krall EA, Dawson-Hughes B. Heritable and life-style determinants of bone mineral density. *J Bone Miner Res* 1993; **8**: 1–9.
6 Gueguen R, Jouanny P, Guillemin F, Kuntz C, Pourel J, Siest G. Segregation analysis and variance components analysis of bone mineral density in healthy families. *J Bone Miner Res* 1995; **10**: 2017–2022.
7 Nelson DA, Kleerekoper M. The search for the osteoporosis gene. *J Clin Endocrinol Metab* 1997; **82**: 989–990.
8 Liu YZ, Liu YJ, Recker RR, Deng HW. Molecular studies of identification of genes for osteoporosis: the 2002 update. *J Endocrinol* 2003; **177**: 147–196.
9 Morrison NA, Qi JC, Tokita A *et al.* Prediction of bone density from vitamin D receptor alleles. *Nature* 1994; **367**: 284–287.
10 Ogawa S, Hosoi T, Shiraki M *et al.* Association of estrogen receptor beta gene polymorphism with bone mineral density. *Biochem Biophys Res Commun* 2000; **269**: 537–541.
11 Uitterlinden AG, Burger H, Huang Q *et al.* Relation of alleles of the collagen type Ialpha1 gene to bone density and the risk of osteoporotic fractures in postmenopausal women. *N Engl J Med* 1998; **338**: 1016–1021.
12 Hosoi T, Miyao M, Inoue S *et al.* Association study of parathyroid hormone gene polymorphism and bone mineral density in Japanese postmenopausal women. *Calcif Tissue Int* 1999; **64**: 205–208.
13 Nusse R, Varmus HE. Wnt genes. *Cell* 1992; **69**: 1073–1087.
14 Barrow JR, Thomas KR, Boussadia-Zahui O *et al.* Ectodermal Wnt3/beta-catenin signaling is required for the establishment and maintenance of the apical ectodermal ridge. *Genes Dev* 2003; **17**: 394–409.
15 Soshnikova N, Zechner D, Huelsken J *et al.* Genetic interaction between Wnt/beta-catenin and BMP receptor signaling during formation of the AER and the dorsal-ventral axis in the limb. *Genes Dev* 2003; **17**: 1963–1968.
16 Cadigan KM, Nusse R. Wnt signaling: a common theme in animal development. *Genes Dev* 1999; **11**: 3286–3305.
17 Tamai K, Semenov M, Kato Y *et al.* LDL-receptor-related proteins in Wnt signal transduction. *Nature* 2000; **407**: 530–535.
18 Mao J, Wang J, Liu B *et al.* Low-density lipoprotein receptor-related protein-5 binds to Axin and regulates the canonical Wnt signaling pathway. *Mol Cell* 2001; **7**: 801–809.
19 Gong Y, Slee RB, Fukai N *et al.* LDL receptor-related protein 5 (LRP5) affects bone accrual and eye development. *Cell* 2001; **107**: 513–523.
20 Kato M, Patel MS, Levasseur R *et al.* Cbfa1-independent decrease in osteoblast proliferation, osteopenia, and persistent embryonic eye vascularization in mice deficient in Lrp5, a Wnt coreceptor. *J Cell Biol* 2002; **157**: 303–314.
21 Boyden LM, Mao J, Belsky J *et al.* High bone density due to a mutation in LDL-receptor-related protein 5. *N Engl J Med* 2002; **346**: 1513–1521.
22 Little RD, Carulli JP, Del Mastro RG *et al.* A mutation in the LDL receptor-related protein 5 gene results in the

autosomal dominant high-bone-mass trait. *Am J Hum Genet* 2002; **70**: 11–19.
23 Bain G, Muller T, Wang X, Papkoff J. Activated beta-catenin induces osteoblast differentiation of C3H10T1/2 cells and participates in BMP2 mediated signal transduction. *Biochem Biophys Res Commun* 2003; **301**: 84–91.
24 Wang S, Krinks M, Lin K, Luyten FP, Moos M Jr. Frzb, a secreted protein expressed in the Spemann organizer, binds and inhibits Wnt-8. *Cell* 1997; **88**: 757–766.
25 Leyns L, Bouwmeester T, Kim SH, Piccolo S, De Robertis EM. Frzb-1 is a secreted antagonist of Wnt signaling expressed in the Spemann organizer. *Cell* 1997; **88**: 747–756.
26 James IE, Kumar S, Barnes MR *et al.* FrzB-2: a human secreted frizzled-related protein with a potential role in chondrocyte apoptosis. *Osteoarthritis Cartilage* 2000; **8**: 452–463.
27 Urano T, Yashiroda H, Muraoka M *et al.* p57 (Kip2) is degraded through the proteasome in osteoblasts stimulated to proliferation by transforming growth factor beta1. *J Biol Chem* 1999; **274**: 12197–12200.
28 Asai T, Ohkubo T, Katsuya T *et al.* Endothelin-1 gene variant associates with blood pressure in obese Japanese subjects: the Ohasama Study. *Hypertension* 2001; **38**: 1321–1324.
29 Nefussi JR, Boy-Lefevre ML, Boulekbache H, Forest N. Mineralization in vitro of matrix formed by osteoblasts isolated by collagenase digestion. *Differentiation* 1985; **29**: 160–168.
30 Bellows CG, Aubin JE, Heersche JN, Antosz ME. Mineralized bone nodules formed in vitro from enzymatically released rat calvaria cell populations. *Calcif Tissue Int* 1986; **38**: 143–154.
31 Aubin JE. Advances in the osteoblast lineage. Biochem. *Cell Biol* 1998; **76**: 899–910.
32 Eastman Q, Grosschedl R. Regulation of LEF-1/TCF transcription factors by Wnt and other signals. *Curr Opin Cell Biol* 1999; **11**: 233–240.
33 Berndt T, Craig TA, Bowe AE *et al.* Secreted frizzled-related protein 4 is a potent tumor-derived phosphaturic agent. *J Clin Invest* 2003; **112**: 785–794.

JOURNAL OF CELLULAR PHYSIOLOGY 203:193–201 (2005)

Survival Versus Apoptotic 17β-Estradiol Effect: Role of ERα and ERβ Activated Non-genomic Signaling

FILIPPO ACCONCIA,[1] PIERANGELA TOTTA,[1] SUMITO OGAWA,[2] IRENE CARDILLO,[1] SATOSHI INOUE,[2] STEFANO LEONE,[1] ANNA TRENTALANCE,[1] MASAMI MURAMATSU,[2] AND MARIA MARINO[1]*

[1]*Department of Biology, University "Roma Tre," Rome, Italy*
[2]*Research Center for Genomic Medicine, Saitama Medical School, Saitama, Japan*

The capability of 17β-estradiol (E2) to induce the non-genomic activities of its receptors (ERα and ERβ) and to evoke different signaling pathways committed to the regulation of cell proliferation has been analyzed in different cell cancer lines containing transfected (HeLa) or endogenous (HepG2, DLD1) ERα or ERβ. In these cell lines, E2 induced different effects on cell growth/apoptosis in dependence of ER isoforms present. The E2–ERα complex rapidly activated multiple signal transduction pathways (i.e., ERK/MAPK, PI3K/AKT) committed to both cell cycle progression and apoptotic cascade prevention. On the other hand, the E2–ERβ complex induced the rapid and persistent phosphorylation of p38/MAPK which, in turn, was involved in caspase-3 activation and cleavage of poly(ADP-ribose)polymerase, driving cells into the apoptotic cycle. In addition, the E2–ERβ complex did not activate any of the E2–ERα-activated signal molecules involved in cell growth. Taken together, these results demonstrate the ability of ERβ isoform to activate specific signal transduction pathways starting from plasma membrane that may justify the effect of E2 in inducing cell proliferation or apoptosis in cancer cells. In particular this hormone promotes cell survival through ERα non-genomic signaling and cell death through ERβ non-genomic signaling. J. Cell. Physiol. 203: 193–201, 2005.

Knowledge of the molecular mechanism by which estrogens exert pleiotropic functions in different tissues and organs has evolved rapidly during the past two decades. In particular, the mechanism by which 17β-estradiol (E2) induces cell proliferation has been the object of extensive studies in several tissues (Sutherland et al., 1983; Marino et al., 1998, 2001; Castoria et al., 1999, 2001; Razandi et al., 1999). However, recent reports demonstrated that E2 could even decrease cell growth by significantly increasing apoptosis in breast cancer MCF-7 cell variants, prostate cells, and several other cell types (see Song and Santen, 2003 for review). Whether the E2 apoptotic effects can be explained by the expression of different estrogen receptor (ER) isoforms (i.e., ERα and ERβ) is presently unknown.

It has been assumed that E2 exerts survival proliferative effects mainly by rapid non-genomic mechanisms originating from the hormone binding to ERα (Marino et al., 1998, 2002; Castoria et al., 1999, 2001; Lobenhofer et al., 2000; Fernando and Wimalasena, 2004). In line with this assumption, E2 treatment of MCF-7 cells triggers association of ERα with Src kinase and p85, the regulatory subunit of PI3K, leading to DNA synthesis (Castoria et al., 2001). Moreover, E2 induces rapid non-genomic pathways and DNA synthesis even in ERα transiently transfected cell lines (e.g., Chinese hamster ovary, CHO; cervix epitheloid carcinoma cell line, HeLa) (Razandi et al., 1999; Marino et al., 2002). In addition, multiple and parallel signal transduction pathways are rapidly activated by the E2–ERα complex in hepatoma, HepG2, cells (e.g., ERK/MAPK, PI3K/AKT) (Marino et al., 2003). The disruption of such membrane starting pathways completely prevents the E2-induced DNA synthesis and the cyclin D_1 expression at the specific response elements, activator protein-1 (AP-1) and stimulating protein-1 (SP-1) (Marino et al., 2002, 2003). All these results point to the concept that ERα is the primary endogenous mediator of rapid E2 actions committed to cell proliferation.

Less information is available on the role played by ERβ in E2 proliferative effects. Data from cell cultures, gene expression, and knockout mice clearly indicate that E2-activated ERβ may function as a tumor suppressor by modulating the proliferative effects of ERα (Couse and Korach, 1999; Weihua et al., 2003; Cheng et al., 2004; Paruthiyil et al., 2004, Strom et al., 2004). These studies support a functional antagonism between ERα and ERβ with respect to the E2-induced cell proliferation, but do not clarify either the putative role of ERβ in E2-induced apoptosis or the signal transduction pathways involved. However, the ability of E2–ERβ complex to activate rapid non-genomic mechanisms has been reported. A subpopulation of ERβ transfected into CHO cells is membrane bound and capable of activating IP_3 production, ERK/MAPK and c-Jun kinase phosphorylation (Razandi et al., 1999). Recently, Geraldes and coworkers (Geraldes et al., 2003) reported that E2 reduces ERK/MAPK activity through ERβ stimulation in porcine smooth muscle cells. Moreover, conflicting

Abbreviations: E2, 17β-estradiol; E2-BSA, β-estradiol 6-(o-carboxy-methyl)oxime:BSA; ER, estrogen receptor; ERE, estrogen responsive element; ERK, extracellular regulated kinase; MAPK, mitogen-activated protein kinase; PI3K, phosphoinositide-3-kinase; PKC, protein kinase C; PARP, poly(ADP-ribose) polymerase.

Contract grant sponsor: MURST; Contract grant sponsor: University "Roma Tre"; Contract grant number: RBAU01TXN3_001; Contract grant sponsor: FIRB 2001 and 2004 University "Roma Tre".

*Correspondence to: Maria Marino, Department of Biology, University "Roma Tre," Viale G. Marconi, 446, I-00146 Rome, Italy. E-mail: m.marino@uniroma3.it

Received 4 June 2004; Accepted 29 July 2004

DOI: 10.1002/jcp.20219

evidences on the ability of ERβ to activate or inactivate Src and p38 kinases (Castoria et al., 2001; Kousteni et al., 2001; Geraldes et al., 2003; Mori-Abe et al., 2003) has been also reported. In particular, the existence of non-genomic mechanism(s) underling the antiproliferative effects of E2–ERβ complex is to date completely unknown.

Here, the ability of E2 to induce ERs activities has been studied in the HeLa cells devoid of any ERs and rendered E2-sensitive by transient transfection with human ERα or ERβ expression vectors. We report that E2 induced different effects on cell growth/apoptosis decision in the presence of the two different isoforms of receptor. The E2–ERα complex activated multiple signal transduction pathways (i.e., ERK/MAPK, PI3K/AKT, p38/MAPK) involved in cell cycle progression, whereas the E2–ERβ complex activated only p38/MAPK, which in turn, drives cells to apoptosis. A role of E2-induced ERK/MAPK activation in regulating some steps of the pro-apoptotic pathways is also demonstrated. These results were confirmed also in cancer cell lines expressing endogenous level of ERα or ERβ. Altogether our findings indicate a new action mechanism for the E2–ERβ complex pointing to the role of E2-induced rapid non-genomic signals in driving cell proliferation or apoptosis in cancer cells.

MATERIALS AND METHODS

Reagents

17β-estradiol, 17α-estradiol, L-glutamine, gentamicin, penicillin, RPMI-1640 and DMEM (without phenol red), charcoal-stripped fetal calf serum, and estradiol-BSA conjugate (β-estradiol 6-(o-carboxy-methyl)oxime:BSA, E2-BSA) were purchased from Sigma Chemical Co. (St. Louis, MO). The estrogen receptor inhibitor ICI 182,780 was obtained from Tocris (Ballwin, MO). The ERK/MAPK cascade inhibitor, U 0126, the PI3K inhibitor, Ly 294002, and the p38/MAPK inhibitor, SB 203580, were obtained from Calbiochem (San Diego, CA). Lipofectamine reagent was obtained from GIBCO-BRL Life-technology (Gaithersburg, MD). The luciferase kit was obtained from Promega (Madison, WI). GenElute plasmid maxiprep kit was obtained from Sigma Chemical Co. Bradford Protein Assay was obtained from BIO-RAD Laboratories (Hercules, CA). The policlonal anti-phospho-AKT, anti-phospho-p38, and anti-p38 antibodies were obtained by New England Biolabs (Beverly, MA); the policlonal anti-ERα, anti-ERβ, and anti-ERK and the monoclonal anti-phospho-ERK, anti-AKT, anti-Bcl-2, anti-caspase-3, anti-poly(ADP-ribose) polymerase (PARP), and anti-actin antibodies were obtained from Santa Cruz Biotechnology (Santa Cruz, CA). CDP-Star, chemiluminescence reagent for Western blot was obtained from NEN (Boston, MA).

All the other products were from Sigma Chemical Co. Analytical or reagent grade products, without further purification, were used.

Cell culture

The ER devoid human cervix epitheloid carcinoma cell line (HeLa) (Marino et al., 2002), the ERα containing hepatoma cell line (HepG2) (Marino et al., 2002, 2003; Moon et al., 2004), and the ERβ containing human colon adenocarcinoma cells (DLD1) (Fiorelli et al., 1999; Di Leo et al., 2001) were used as experimental models. Cells were routinely grown in air containing 5% CO_2 in modified, phenol red-free, DMEM (HeLa cells) or RPMI-1640 (HepG2 and DLD1 cells) media, containing 10% (v/v) charcoal-stripped fetal calf serum, L-glutamine (2 mM), gentamicin (0.1 mg/ml), and penicillin (100 U/ml). Cells were passaged every 2 days (HeLa and DLD1 cells) or every 4 days (HepG2 cells) and media changed every 2 days.

Plasmids and transfection procedures

The expression vectors for pCR3.1-β-galactosidase, human ERα (pSG5-HE0) (Marino et al., 2003), and human ERβ (pCNX2-ERβ) (Ogawa et al., 1998) have been used. Furthermore an empty vector, pCMV5, was used as control (Marino et al., 2001). Plasmids were purified for transfection using a plasmid preparation kit according to manufacturer's instructions. A luciferase dose response curve showed that the maximum effect was present when 1 μg of DNA was transfected in HeLa cells together with 1 μg of pCR3.1-β-galactosidase to normalize transfection efficiency (~55–65%). HeLa cells were grown to ~70% confluence, then transfected using Lipofectamine Reagent according to the manufacturer's instructions. Six hours after transfection the medium was changed and 24 h thereafter cells were stimulated with 10 nM E2.

Cell viability and cell cycle

HeLa cells were grown to ~70% confluence in 6-well plates, then transfected and, after 24 h, stimulated. At different times after treatment cells were harvested with trypsin and centrifuged. Cells were stained with trypan blue solution and counted in a hemocytometer (improved Neubauer chamber) in quadruplicate. For the cell cycle analysis, 10^6 cells were fixed with 1 ml ice-cold 70% ethanol and subsequently stained with 2 μg/ml DAPI/PBS solution. The fluorescence of DNA was measured with a DAKO Galaxy flow cytometer equipped with HBO mercury lamp and the percentage of cells present in sub-G1, G1, S, and G2/M phases was calculated using a FloMax© Software.

Electrophoresis and immunoblotting

Stimulated and un-stimulated cells were lysed as described (Marino et al., 1998). When indicated 1 μM ICI 182,780 or 10 μM U 0126 or 10 μM Ly 294002 or 5 μM SB 203580 were added to the medium 15 or 30 min, respectively, before agonist stimulation. Cells were solubilized in 0.125 M Tris-HCl (pH 6.8) containing 10% SDS (w/v), 1 mM phenylmethylsulfonyl fluoride, and 5 μg/ml leupeptin and boiled for 2 min. Proteins were quantified using the Bradford Protein Assay (Bradford, 1976). Twenty microgram solubilized proteins were resolved using SDS–PAGE at 100 V for 1 h. The proteins were then electrophoretically transferred to nitrocellulose for 45 min at 100 V at 4°C. The nitrocellulose was treated with 3% bovine serum albumin in 138 mM NaCl, 26.8 mM KCl, 25 mM Tris-HCl (pH 8.0), 0.05% Tween-20, 0.1% BSA, and then probed at 4°C overnight with either one of anti-ERα, anti-ERβ, anti-phospho-ERK, anti-phospho-AKT, anti-phospho-p38, anti-caspase-3, anti-Bcl-2, or anti-PARP antibodies. The nitrocellulose was stripped by Restore Western Blot Stripping Buffer (Pierce Chemical Company, Rockford, IL) for 10 min at room temperature and then probed with either anti-ERK, anti-AKT, or anti-p38 antibodies (1 μg/ml). Anti-actin antibody (1 μg/ml) was used to normalize the sample loading. Antibody reaction was visualized with chemiluminescence reagent for Western blot.

RESULTS

Divergent effects of E2 in inducing cell growth in the presence of ERα or ERβ

The level of exogenous ERα or ERβ was assessed in HeLa cells untrasfected (none) or transfected with either empty, ERα, or ERβ expression vectors. The Western blot analysis (Fig. 1a) confirmed the absence of ERs in both un-transfected and empty vector-transfected HeLa cells, whereas a unique band at 67 kDa (ERα-containing HeLa cells) or at 57 kDa (ERβ-containing HeLa cells) was detected. The time course of growth of HeLa cells transfected with empty plasmid or ERα or ERβ expression vectors was examined in the presence of E2 and in the presence of the ER inhibitor ICI 182,780. Figure 1b shows that the growth of empty plasmid-transfected HeLa cells was not affected by E2 or ICI 182,780 suggesting that the presence of ER is necessary for the hormone effects. On the other hand, E2 was mitogen for ERα-transiently transfected HeLa cells (Fig. 1c), whereas a decrease in growth was detected after E2 stimulation in ERβ-transfected HeLa cells with respect to unstimu-

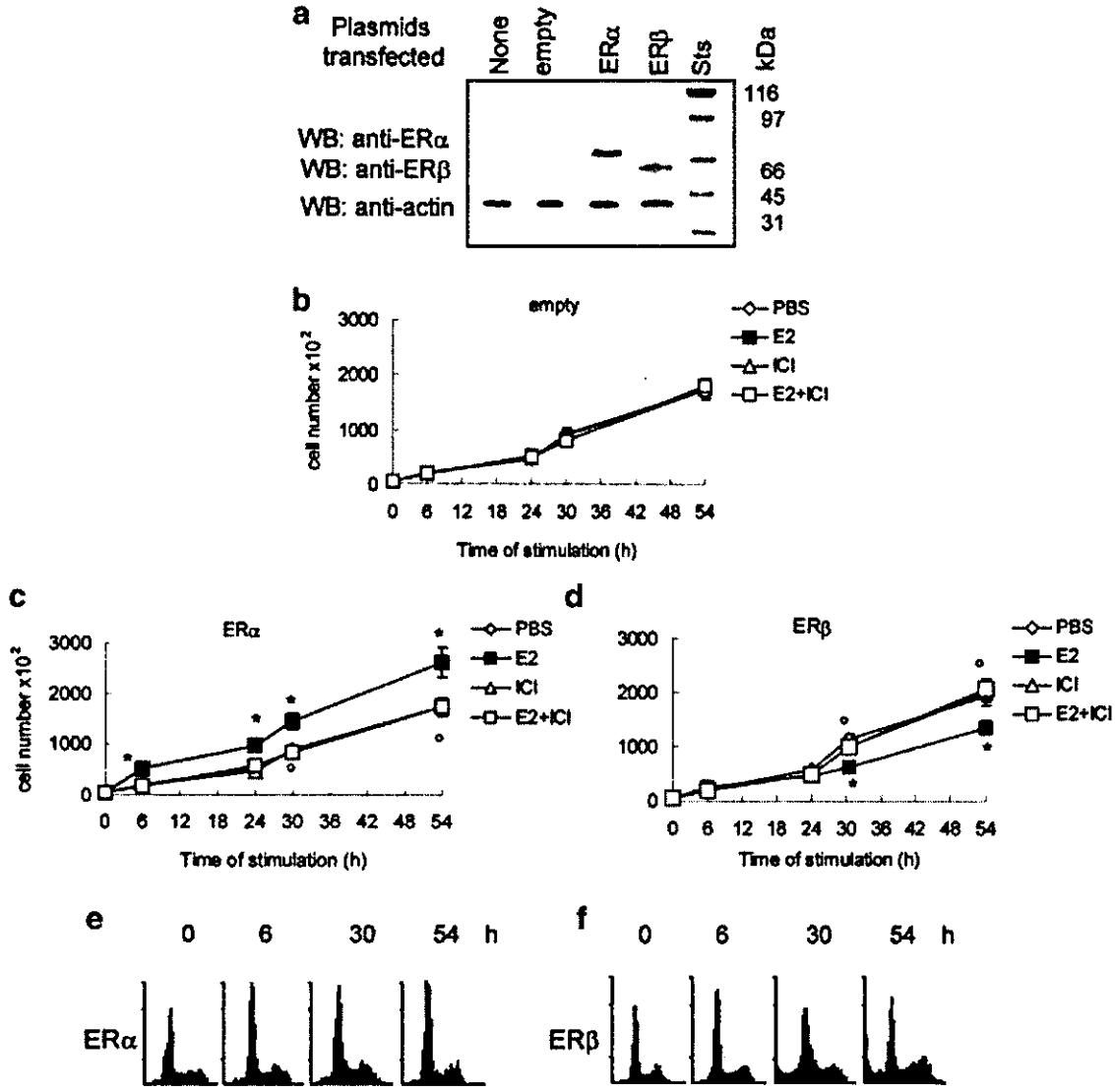

Fig. 1. Level of estrogen receptors (ERs) in transfected and un-transfected and time course of HeLa cell growth in the presence of 17β-estradiol (E2). Western blot analysis of ERα and ERβ levels were performed in un-transfected (none) or transfected HeLa cells with either empty, human ERα or human ERβ expression vectors (**part a**). HeLa cells transfected with empty (**part b**) or human ERα (**part c**) or human ERβ (**part d**) expression vectors were grown in DMEM in the presence of E2 (10 nM) and/or ICI 182,780 (ICI, 1 μM) counted at the indicated times. The data are the mean values ± SD of five independent experiments carried out in duplicate. $P < 0.001$, calculated with Student's t-test, compared with respective un-stimulated values (PBS) (*) or with E2-stimulated values (°). Flow cytometric analysis of the HeLa cells transfected with human ERα (**part e**) or human ERβ (**part f**) vectors after different time of E2-treatment compared with un-stimulated cells (0). The plots indicate cell cycle distribution present in sub-G1, G1, S, and G2/M phases, respectively. For details see the text.

lated ones (Fig. 1d). The cell pre-treatment with the ER inhibitor ICI 182,780 completely blocked the E2 effects both in ERα- and in ERβ-embedded HeLa cells. Further, we analyzed, by flow cytometry, the HeLa cell cycle distribution at different time after treatment. The typical plot of plasmid transfected-HeLa cell population is illustrated in Figure 1e and f (0 h). The first peak indicates the cell number in G1 phase of the cell cycle (50.0 ± 5.0%) followed by S phase (16.3 ± 3.2%), and by the peak of G2/M phase (19.8 ± 2.8%). Increasing the time of E2-stimulation (Fig. 1e; 6, 30, and 54 h), the number of cells in G1 phase of cell cycle increased reaching 65.4 ± 3.8% 54 h after the hormone administration to HeLa cells expressing ERα. On the contrary, when HeLa cells were endowed with ERβ (Fig. 1f; 6, 30, and 54 h), the number of cells in sub-G1 region increased reaching 9.5 ± 1.0% 54 h after the E2 stimulation thus suggesting the presence of DNA fragmentation.

Divergent effects of E2 in inducing an apoptotic cascade in the presence of ERα or ERβ

To determine whether the reported increase of cell population in the sub-G1 phase was truthfully related to the induction of an apoptotic cascade, we analyzed the cleavage of the caspase-3 proform (32-kDa band) which results in the production of the active subunit of the protease (17-kDa band). Caspase-3 proform was expressed in HeLa cells transfected with empty or ERα or ERβ expression vectors (Fig. 2a). No cleavage of caspase-3 was induced by E2 in empty or ERα-containing HeLa cells whereas E2 induced the production of the active subunit in the presence of ERβ.

To confirm that the appearance in the 17-kDa band was associated with an increase in caspase-3 activity, we analyzed one of the known substrates of caspase-3, PARP. This 116-kDa, DNA repair enzyme, is cleaved by

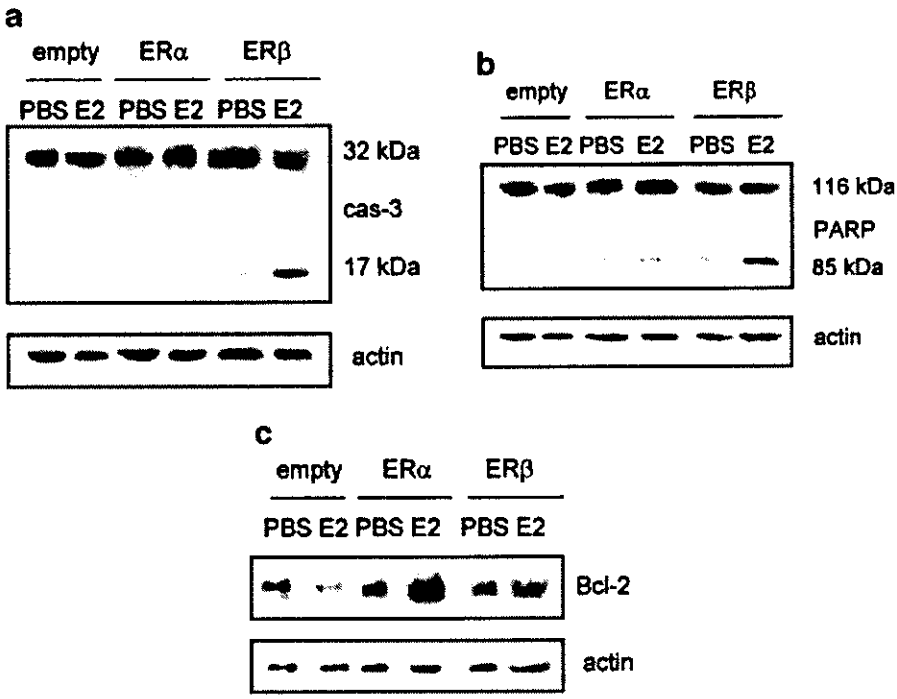

Fig. 2. Effect of E2 in the induction of pro-apoptotic proteins. Western blot analysis of caspase-3 (**part a**), PARP (**part b**) activation, and Bcl-2 (**part c**) levels were performed, as described in "Materials and Methods," on un-stimulated (PBS) and 24 h E2-treated (10 nM) HeLa cells transfected with human ERα, human ERβ, or empty expression vectors. The amounts of protein levels were normalized by comparison with actin expression. Typical blot of three independent experiments. For details see the text.

the caspase-3 producing the inactive 85-kDa fragment (Fig. 2b). By Western blot analysis, treatment of empty- and ERα-containing HeLa cells with E2 did not induce any conversion of PARP in the inactive form. On the contrary, the treatment of ERβ-transfected HeLa cells with E2 resulted in the conversion of PARP into the inactive 85-kDa fragment. These results were consistent with the idea that, in the presence of ERβ, E2 specifically induced an apoptotic cascade involving the caspase-3 activation and a downstream substrate like PARP. This was further confirmed by the expression of Bcl-2 level, the survival factor that can block both necrotic and apoptotic cell death (Dubal et al., 1999). Only the treatment of ERα-transfected HeLa cells with E2 markedly increased the amount of Bcl-2 (Fig. 2c).

Signal transduction pathways involved in the E2-induced apoptotic cascade

We previously reported that the rapid E2-induced activation of ERK/MAPK and PI3K/AKT pathways is sufficient and necessary for E2-induced cell cycle progression (i.e., DNA synthesis and the transcription of cyclin D_1 gene) (Marino et al., 2002, 2003). Then we asked if the inhibition of these rapid signals was involved in the E2–ERβ-induced apoptotic cascade.

No activation of signal transduction proteins was detected in cells transfected with empty vector and stimulated with E2 (data not shown). However, E2 increased ERK and AKT phosphorylation in HeLa cells transiently transfected with ERα (Fig. 3a). After reprobing the membranes using total ERK or AKT antibodies, to recognize the non-phosphorylated form of these proteins, the specific alteration of signaling proteins by E2 was confirmed to occur in the absence of changes in their expression levels (Fig. 3a). On the other hand, E2 failed to elicit any changes in the phosphorylation or expression level of ERK and AKT in cell expressing ERβ (Fig. 3a). Interestingly, a similar activation was observed in cancer cell lines which express endogenous ERα (HepG2) or ERβ (DLD1). In fact, E2 induced the rapid increase of ERK and AKT phosphorylation only in HepG2 cells (Fig. 3b) whereas it was ineffective in DLD1 cells (Fig. 3c). The level of endogenous ERα or ERβ was assessed in HepG2 and DLD1 cells. The Western blot analysis (Fig. 3d) confirmed the presence of a unique band at 67 kDa (HepG2 cells) or at 57 kDa (DLD1 cells) corresponding to ERα or ERβ, respectively.

Generally, the activation of PI3K/AKT and ERK/MAPK pathways causes cell survival in response to many mitogens and growth factors, whereas the activation of p38/MAPK has been associated with the regulation of apoptosis and differentiation processes (Ambrosino and Nebreda, 2001; Harper and LoGrasso, 2001; Talapatra and Thompson, 2001; Shimada et al., 2003; Porras et al., 2004). To verify this possibility, the effect of E2 on p38/MAPK activation was evaluated. A time course of E2-induced p38/MAPK phosphorylation in HeLa cells transfected with ERα or ERβ is shown in Figure 4a. A rapid and transient increase of p38/MAPK phosphorylation was detected from 15 to 30 min after E2 stimulation in ERα-transfected HeLa cells; whereas E2 induced a rapid (15 min) and persistent (24 h) increase of p38/MAPK phosphorylation in ERβ expressing HeLa cells. In the same way, E2 evoked a rapid (15 min) and transient activation of p38/MAPK in ERα-encoding HepG2 cells (Fig. 4b, upper part) and a rapid and persistent (24 h) phosphorylation of p38/MAPK in ERβ-containing DLD1 cells (Fig. 4b, lower part). Note that, the E2-induced p38/MAPK activation was prevented by the pure anti-ER ICI 182,780 in either cell lines (Fig. 4b). The same inhibitor completely

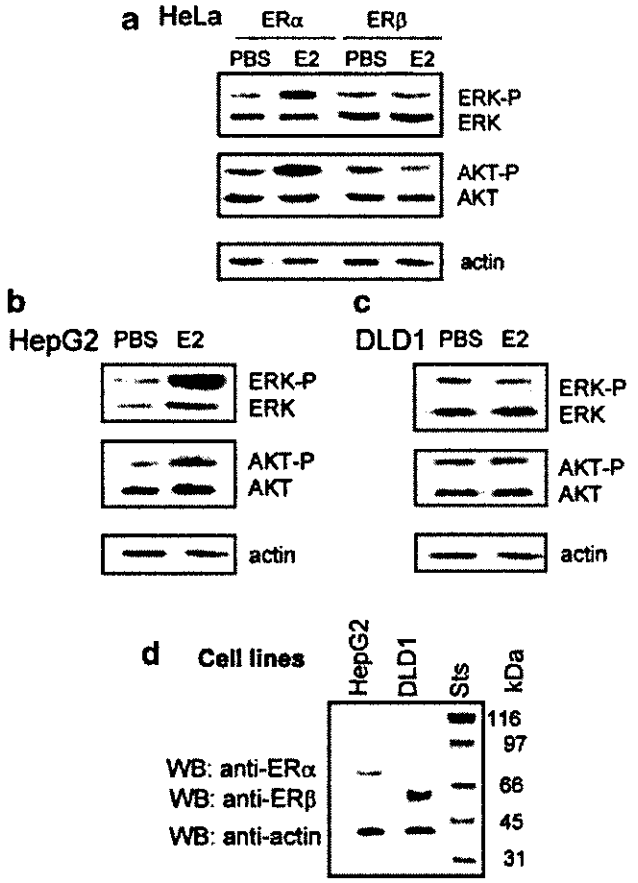

Fig. 3. Signal transduction pathways activated by E2. Western blot analysis of phosphorylated and un-phosphorylated ERK and AKT were performed, as described in "Materials and Methods," on unstimulated (PBS) and 15 min E2-treated (10 nM) HeLa cells transfected with human ERα or human ERβ expression vectors (**part a**) or HepG2 cells (**part b**) or DLD1 cells (**part c**). Western blot analysis of ERα and ERβ levels were performed in HepG2 cells and DLD1 cells (**part d**). The amount of protein levels were normalized by comparison with actin expression. Typical blot of three independent experiments. For details see the text.

prevented the rapid (15 min) E2-induced p38/MAPK phosphorylation also in ER-transfected HeLa cells (Fig. 4c). Furthermore, the E2 inactive stereoisomer, 17α-estradiol, failed to induce p38/MAPK phosphorylation (Fig. 4c), whereas the E2 cell membrane impermeable, E2-BSA (Zheng et al., 1996; Marino et al., 2003), affected the p38/MAPK activation comparably to E2 (Fig. 4c). Altogether these data imply a membrane ER in the rapid and specific E2-induced activation of p38/MAPK signaling.

Cross-talk between proliferative and apoptotic signal transduction pathways and role of E2-induced p38/MAPK

The ability of E2 to induce p38/MAPK phosphorylation even in the presence of ERα was surprising and did not clarify the putative involvement of this kinase in the E2-induced apoptosis. Thus, we asked whether ERK/MAPK and PI3K/AKT cross-talk with p38/MAPK. None of the specific pathway inhibitors used (i.e., Ly 294002 and U 0126) prevented the E2-induced p38/MAPK phosphorylation in ERα-transfected HeLa cells (Fig. 5a) suggesting that the activation of this pathway was parallel and independent on ERK and AKT activation. On the contrary, the cell pre-treatment with the same inhibitors rescued the activation of the pro-apoptotic caspase-3 (Fig. 5b) as well as completely prevented E2-induced, anti-apoptotic, Bcl-2 accumulation (Fig. 5c). The same results were obtained in HepG2 cells (Fig. 5 d, e, and f) further indicating that E2–ERα-induced ERK and AKT activation negatively modulates the apoptotic signals. To direct evaluate the role of p38 in these effects in some experiments cells were pre-treated with the specific p38/MAPK inhibitor, SB 203580 (5 μM), before E2 stimulation. A block of p38/MAPK phosphorylation was evidenced while no effect was present on Bcl-2 levels in both cell lines considered. Note that, caspase-3 cleavage induced by E2 in the presence of U0126 was prevented by the pre-treatment of HepG2 cells with p38/MAPK inhibitor, SB 203580 (30 min) (Fig. 5g). However, the cell pretreatment with the signaling pathways inhibitors alone did not modify the p38/MAPK phosphorylation or caspase-3 and PARP cleavage.

Finally, the pre-treatment of ERβ-transfected HeLa cells with the specific p38/MAPK inhibitor, SB 203580, completely prevented the formation of the caspase-3 active fragment (Fig. 6a) and the cleavage of PARP (Fig. 6b) linking the p38/MAPK activation directly to the apoptosis. As expected, E2 induced p38/MAPK-dependent caspase-3 activation in ERβ-containing DLD1 cells (Fig. 6c) sustaining a pivotal role of the signaling activated by E2–ERβ complex (i.e., prolonged p38/MAPK phosphorylation) in inducing the apoptotic cascade.

DISCUSSION

E2 is known to support cell survival or induce cell death/apoptosis depending on the cell context (Song et al., 2001; Song and Santen, 2003). The mechanism(s) underling these opposite E2 effects could involve the classical/transcriptional mechanism of ER isoforms which, as ligand-dependent transcription factors, modulate the transcription of E2-induced target genes. In addition to this accepted model for the E2 action mechanism, emerging evidences indicated that rapid/non-genomic signaling molecules originating from the cell membrane are involved at least in E2–ERα-induced cell proliferation/survival (Castoria et al., 1999; Razandi et al., 1999, 2000a; Kousteni et al., 2001; Marino et al., 2001, 2002, 2003). These evidences prompted us to examine the non-genomic signaling mechanism(s) generated by the E2–ERβ complex and to compare the role(s) played by these rapid signals with those generated after E2–ERα binding. Although the different functions of ERα versus ERβ on cell proliferation/apoptosis balance has been suggested (Matthews and Gustafsson, 2003; Weihua et al., 2003), the contribution of signal transduction pathways generated by each isoform on these E2-induced cellular functions has not been yet clarified. Therefore, we chose the ER-devoid HeLa cells as experimental model. The transiently transfected HeLa cells allow us to discriminate the effect of each ER isoforms, without the mutual interference, in a E2-induced proliferation model (Marino et al., 2001, 2002). Furthermore, to avoid any dilemma due to the receptors over-expression, some experiments were performed in parallel in two different cancer cell lines which express endogenous ERα (HepG2) (Marino et al., 2001, 2002, 2003; Moon et al., 2004) or ERβ (DLD1) (Fiorelli et al., 1999; Di Leo et al., 2001).

In these experimental conditions, E2 induced different effects on cell growth or apoptosis in dependence on ER isoform present. While the E2–ERα complex activated multiple signal transduction pathways committed to